USGS
science for a changing world

Prepared in cooperation with Bureau of Reclamation

Trends in Recent Historical and Projected Climate Data for the Colorado River Basin and Potential Effects on Groundwater Availability

Scientific Investigations Report 2020–5107

U.S. Department of the Interior
U.S. Geological Survey

Cover. Map of the Colorado River Basin, western United States and northern Mexico

Trends in Recent Historical and Projected Climate Data for the Colorado River Basin and Potential Effects on Groundwater Availability

By Fred D Tillman, Subhrendu Gangopadhyay, and Tom Pruitt

Prepared in cooperation with Bureau of Reclamation

Scientific Investigations Report 2020–5107

U.S. Department of the Interior
U.S. Geological Survey

U.S. Department of the Interior
DAVID BERNHARDT, Secretary

U.S. Geological Survey
James F. Reilly II, Director

U.S. Geological Survey, Reston, Virginia: 2020

For more information on the USGS—the Federal source for science about the Earth, its natural and living resources, natural hazards, and the environment—visit https://www.usgs.gov or call 1–888–ASK–USGS.

For an overview of USGS information products, including maps, imagery, and publications, visit https://store.usgs.gov.

Suggested citation:
Tillman, F.D., Gangopadhyay, S., and Pruitt, T., 2020, Trends in recent historical and projected climate data for the Colorado River Basin and potential effects on groundwater availability: U.S. Geological Survey Scientific Investigations Report 2020–5107, 24 p., https://doi.org/10.3133/sir20205107.

Associated data for this publication:
Tillman, F.D., Gangopadhyay, S., and Pruitt, T., 2019, Soil-water balance groundwater infiltration model results for the Lower Colorado River Basin: U.S. Geological Survey data release, https://doi.org/10.5066/P9VLU0O6.

Tillman, F.D., 2017, Soil-water balance groundwater recharge model results for the upper Colorado River Basin [ver. 2.0, April 2017]: U.S. Geological Survey data release, https://doi.org/10.5066/F7ST7MX7.

ISSN 2328-0328 (online)

Acknowledgments

This investigation of recent historical and projected climate data for the Colorado River Basin and potential effects on groundwater availability was supported by the Bureau of Reclamation's Science and Technology and WaterSMART (Sustain and Manage America's Resources for Tomorrow) Programs.

Contents

Figures

Table

Conversion Factors

U.S. customary units to International System of Units

Multiply	By	To obtain
	Length	
centimeter (cm)	0.3937	inch (in.)
millimeter (mm)	0.03937	inch (in.)
meter (m)	3.281	foot (ft)
kilometer (km)	0.6214	mile (mi)
kilometer (km)	0.5400	mile, nautical (nmi)
meter (m)	1.094	yard (yd)
	Area	
square kilometer (km^2)	247.1	acre
square kilometer (km^2)	0.3861	square mile (mi^2)

Temperature in degrees Celsius (°C) may be converted to degrees Fahrenheit (°F) as

$$°F = (1.8 \times °C) + 32.$$

Temperature in degrees Fahrenheit (°F) may be converted to degrees Celsius (°C) as

$$°C = (°F - 32) / 1.8.$$

Datum

Vertical coordinate information is referenced to the North American Vertical Datum of 1988 (NAVD 88).

Abbreviations

APWL	accumulated potential water loss
AET	actual evapotranspiration
BCSD	Bias-Correction and Spatial Disaggregation method
CMIP	Coupled Model Intercomparison Project
DEM	digital elevation model
EPA	U.S. Environmental Protection Agency
GCM	global climate model
GHCN	Global Historical Climatology Network
HUC	hydrologic unit code
LOCA	Localized Constructed Analog
NRCS	National Resources Conservation Service
PET	potential evapotranspiration
RCP	Representative Concentration Pathway
SWB	Soil-Water-Balance
USGS	U.S. Geological Survey

Trends in Recent Historical and Projected Climate Data for the Colorado River Basin and Potential Effects on Groundwater Availability

By Fred D Tillman,[1] Subhrendu Gangopadhyay,[2] and Tom Pruitt[2]

Abstract

Understanding recent historical and projected trends in precipitation and temperature in the Colorado River Basin, and estimating what the projected changes in these climate parameters may mean for groundwater resources in the region, is important for water managers and policymakers to sustainably manage water resources in the basin. Historical (1896–2019) precipitation and temperature data for the upper and lower Colorado River Basins were analyzed to better understand recent trends in climate data that may affect groundwater resources in the area. Historical data indicate multidecadal-scale cyclical patterns in precipitation in both the upper and lower basins. Although upper basin precipitation had no statistical trend over the recent historical period, the lower basin had a weak negative trend over this period. Multidecadal-scale cyclical patterns in temperature also are observed in historical climate data in both the upper and lower basins, at least until the early 1970s. Beginning at that time, both the upper and lower basins experienced strong, monotonic positive trends in temperature. Basic principles of hydrology indicate that periods of decreasing precipitation as well as increasing temperature would have a negative effect, that is, reduction in groundwater infiltration and hence, reduced recharge of aquifer systems.

Projected climate data from 97 Coupled Model Intercomparison Project phase 5 (CMIP5) ensemble members across the full range of Representative Concentration Pathway (RCPs) from water years 1951 through 2099 were evaluated to understand what current global climate models are projecting about future conditions in the Colorado River Basin, and what this might mean for groundwater systems in the region. Precipitation in the upper basin is projected to increase throughout the rest of the century, rising to 6 percent above the 1951–2015 historical period by mid-century and to 9 percent above the historical period by the end of the century. Temperature in the upper basin also is projected to be above the recent historical median throughout the rest of the century, with steady warming in decadal average temperatures expected until the last quarter of this century. In contrast to projected precipitation in the upper basin, precipitation in the lower basin is projected to be the same as, or slightly less than, the historical period throughout most of the rest of this century. Like projected temperature in the upper basin, temperature in the lower basin also is projected to be above the recent historical median throughout the rest of the century. Comparing median projections for all future decades with median results from all historical decades, future precipitation is expected to be greater than that of the past in the upper basin, though no significant difference is projected for precipitation in the lower basin. Significant increases (p-value<0.05) are expected in temperature in both the upper and lower basins.

To estimate the effects of projected precipitation and temperature on groundwater systems in the region, results from the 97 member CMIP5 climate projection ensemble were used as input in a Soil-Water Balance (SWB) groundwater infiltration model for the Colorado River Basin. SWB simulation results indicate that the upper Colorado River Basin is expected to experience decades of above-historical-average groundwater infiltration through the end of the century. For the lower Colorado River Basin, simulated groundwater infiltration is projected to be consistently less than the recent (1951–2015) historical period for most of the remaining century. A comparison of the distribution of all median simulated groundwater infiltration results between recent historical and future periods indicates projected groundwater infiltration in the upper basin is significantly (p-value<0.05) greater over the combined 2020–2099 future period than the recent (1951–2015) historical period. Moreover, in 41 of 71 (58 percent) possible future decades in this century, groundwater infiltration is projected to be greater than the 75th percentile of historical simulated groundwater infiltration. Projected groundwater infiltration in the lower Colorado River Basin across all future decades is significantly less than in the historical period. Of the 71 future decades in the century, projected groundwater infiltration in the

[1]U.S. Geological Survey.

[2]Bureau of Reclamation.

lower basin is expected to be less than the 25th percentile of historical infiltration in 55 (77 percent) of the 10-year periods. Important differences in projected precipitation between the upper (increasing precipitation) and lower (decreasing precipitation) basins largely drive the different responses of simulated groundwater infiltration in the upper (increasing infiltration) and lower (decreasing infiltration) basins. It will be useful to revisit projections in groundwater infiltration in the Colorado River Basin when more up-to-date projections of precipitation become available from the next Coupled Model Intercomparison Project phases or by using climate input developments through Regional Climate Modeling efforts and stochastic weather generators.

Introduction

The Colorado River supplies water to more than 35 million people in the United States and 3 million people in Mexico (Bureau of Reclamation, 2013a; Colorado River Basin Salinity Control Forum, 2013). The Colorado River Basin drains parts of seven U.S. States and Mexico and is divided into upper and lower basins at the compact point of Lee Ferry, Arizona, located 1.6 kilometers (km) downstream of the mouth of the Paria River (fig. 1; Anderson, 2004). The flow of the Colorado River in the lower basin is mostly controlled by releases from Glen Canyon Dam. About 90 percent of the flow in the lower Colorado River at Lake Mead originates in the upper basin (U. S. Geological Survey, 2017). Groundwater discharge to streams makes up an estimated 21–58 percent of the flow in rivers and streams in the upper Colorado River Basin (Miller and others, 2014). Although the importance of lower-basin groundwater to flow in the Colorado River is substantially less than in the upper basin, large agricultural areas and fast-growing communities such as Phoenix and Tucson in the lower basin depend on groundwater to meet water needs. Additionally, important ecosystems in the semi-arid lower basin are sustained by groundwater discharge at spring sites. An understanding of recent trends in climate data, projected change in climate data, and projected change in groundwater infiltration in the Colorado River Basin is essential for the sustainable management of the rivers and aquifers in the region. The SECURE Water Act, passed by Congress in 2009, requires the Bureau of Reclamation to report to Congress every 5 years following the initial 2-year reporting requirement (that is, a first report in 2011) on effects and risks resulting from global climate change with respect to the quantity of water resources located in each major Reclamation River Basin (Bureau of Reclamation, 2011). To help address this reporting requirement, the USGS, in cooperation with the Bureau of Reclamation, completed an investigation analyzing trends in recent historical and current state-of-the-science projected climate data for the Colorado River Basin and potential effects on groundwater availability.

Purpose and Scope

The purpose of this report is to document the data, methods, and results from the investigation of recent historical and projected climate data, and simulated, projected groundwater infiltration in the Colorado River Basin. The study area for this investigation, as described below, comprises the upper Colorado River Basin as defined by USGS two-digit hydrologic unit code (HUC) number 14 and the lower Colorado River Basin as defined by USGS two-digit HUC number 15 within the United States (fig. 1). Climate data analyzed for this study include precipitation and temperature for water years (October–September) 1896 through 2019. Projected climate data include precipitation and temperature for water years 2020 through 2099. Groundwater infiltration is simulated using the Soil-Water Balance groundwater infiltration model (Westenbroek and others, 2018) for water years 2020 through 2099.

Previous Studies

Results from analyses of projected climate data and simulated groundwater infiltration in the upper Colorado River Basin described in this report was previously published by Tillman and others (2016). Several publications within the last 5 years have reported on potential effects of projected climate change on water resources in the western or southwestern United States. Cook and others (2015) project increased drought severity with climate change in the southwest and central plains of western North America. In the Southwest, a reduction in cold season precipitation and an increase in evapotranspiration are expected to reduce soil moisture. Dettinger and others (2015) describe projections for continued and increased warming across the western United States, with continued changes in seasonality of snowmelt and streamflow, and a strong potential for increases in evaporative demands. A series of reports focuses on potential effects of projected climate change on agricultural, rangeland, and forest resources in the southwest, in particular the effect of declining snowpack on available irrigation water (Elias and others, 2016; Elias and others, 2018a,b; Havstad and others, 2018; Steele and others, 2018; Thorne and others, 2018). The most recent National Climate Assessment by the U.S. Global Change Research Program (Gonzalez and others, 2018) describes climate model results that project increased temperatures in the southwestern United States, with subsequent increased evapotranspiration, lower soil moisture, reduced snow cover, and changes in the timing of snowmelt and runoff. Studies of the potential effects of projected climate change on groundwater recharge in the western United States (Meixner and others, 2016; Niraula and others, 2017) indicate potential declines in recharge across aquifers in the southern part of the study area. Prein and others (2016) use observation-based results to support projections of climate models that indicate a substantial increase in droughts and aridity in the Southwest.

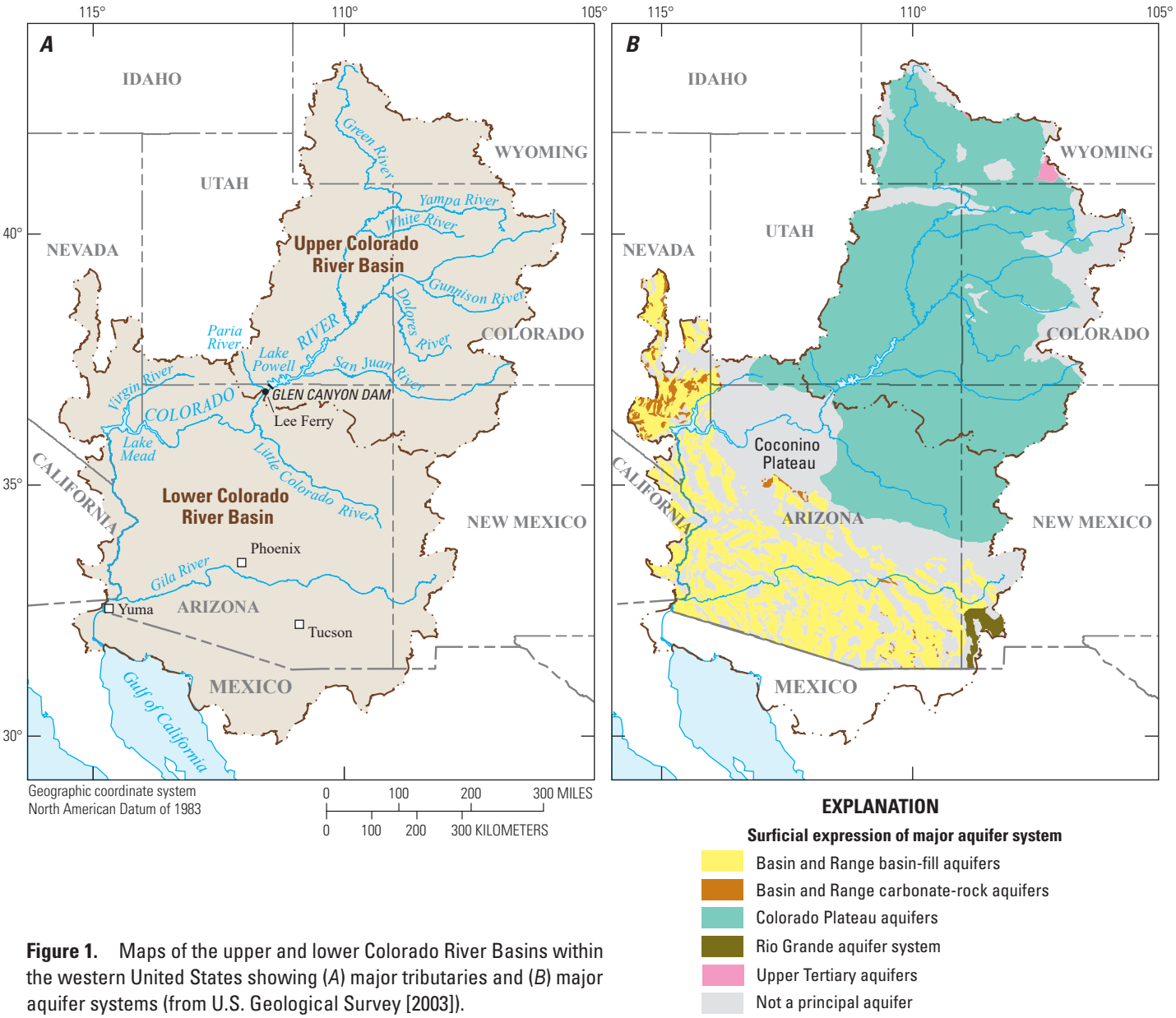

Figure 1. Maps of the upper and lower Colorado River Basins within the western United States showing (*A*) major tributaries and (*B*) major aquifer systems (from U.S. Geological Survey [2003]).

Description of the Study Area

The Colorado River traverses 2,334 km from headwaters in the southern Rocky Mountains of Colorado to the Gulf of California in Mexico (fig. 1). The Colorado River and its tributaries drain an area of 640,000 square kilometers (km^2) in parts of seven U.S. States (Wyoming, Colorado, Utah, New Mexico, Arizona, Nevada, and California) and two Mexican States. The Colorado River Compact of 1922 divided the Colorado River into upper and lower basins at the compact point of Lee Ferry, Arizona—roughly 0.6 km downstream from the mouth of the Paria River (fig. 1). For this study, the Colorado River Basin is defined by Region 14 HUC for the upper Colorado River Basin and Region 15 HUC for the lower Colorado River Basin (see https://water.usgs.gov/GIS/huc.html). Furthermore, only the portion of the Colorado River Basin within the United States (91 percent) is considered in this study, owing to the unavailability of datasets in the Mexican portion of the basin. Major tributaries in the upper basin include the Yampa, Green, White, Gunnison, Dolores, and San Juan Rivers. Major lower basin tributaries include the Little Colorado, Virgin, and Gila Rivers. Land surface elevation in the basin ranges from mountain peaks more than 4,000 meters (m) above the North American Vertical Datum of 1988 (NAVD 88) in the Rocky Mountains to 20 m above NAVD 88 as the Colorado River leaves the United

States near Yuma, Arizona (fig. 2*A*). The climate across the upper and lower basins is also diverse. Average annual precipitation (1981–2010) ranges from more than 1.8 m per year at the highest elevations in the upper basin to as little as 7 centimeters (cm) per year near Yuma, Arizona (fig. 2*B*). Average annual temperatures (1981–2010) are below 0 °C in a few high-elevation locations in the Rocky Mountains and almost 25 °C near Yuma, Arizona (fig. 2*C*). Monthly precipitation in the upper basin is fairly uniform throughout the year, with an average of 28–36 millimeters (mm) per month for all months except June, which receives about 20 mm (fig. 3). Precipitation in the lower basin varies considerably during parts of the year, with 20–30 mm per month from September through March, declining to a low of 7.8 mm in June, then monsoonal storms in July and August result in 44 and 50 mm per month, respectively (fig. 3). Monthly temperature patterns in the upper and lower basins are identical, with lower basin temperatures 7–10 °C warmer than the upper basin (fig. 3). For both the upper and lower basins, average monthly temperatures follow a sinusoidal pattern from highest average temperatures in July to lowest average temperatures in January (fig. 3).

The principal aquifers in the upper basin are the Colorado Plateau regional aquifers that are composed of permeable, moderately to well-consolidated sedimentary rocks ranging in age from Permian to Tertiary (fig. 1; Robson and Banta, 1995), although groundwater in shallow alluvial deposits may be locally important in some locations in the southern Rocky Mountains (Apodaca and Bails, 2000). At least three groups of regional, productive water-yielding geologic units have been identified in the upper basin (Freethey and Cordy, 1991; Robson and Banta, 1995; Geldon 2003a,b). Aquifers contained in Tertiary-age formations of limited extent in the northern and southeastern parts of the basin overlie aquifers in Mesozoic-age formations that also are present throughout most of the study area. Deeper aquifers in Paleozoic-age formations are present throughout much of the upper Colorado River Basin and may rise to land surface in uplifted areas. The Triassic-age Chinle and Moenkopi Formations (confining units) limit

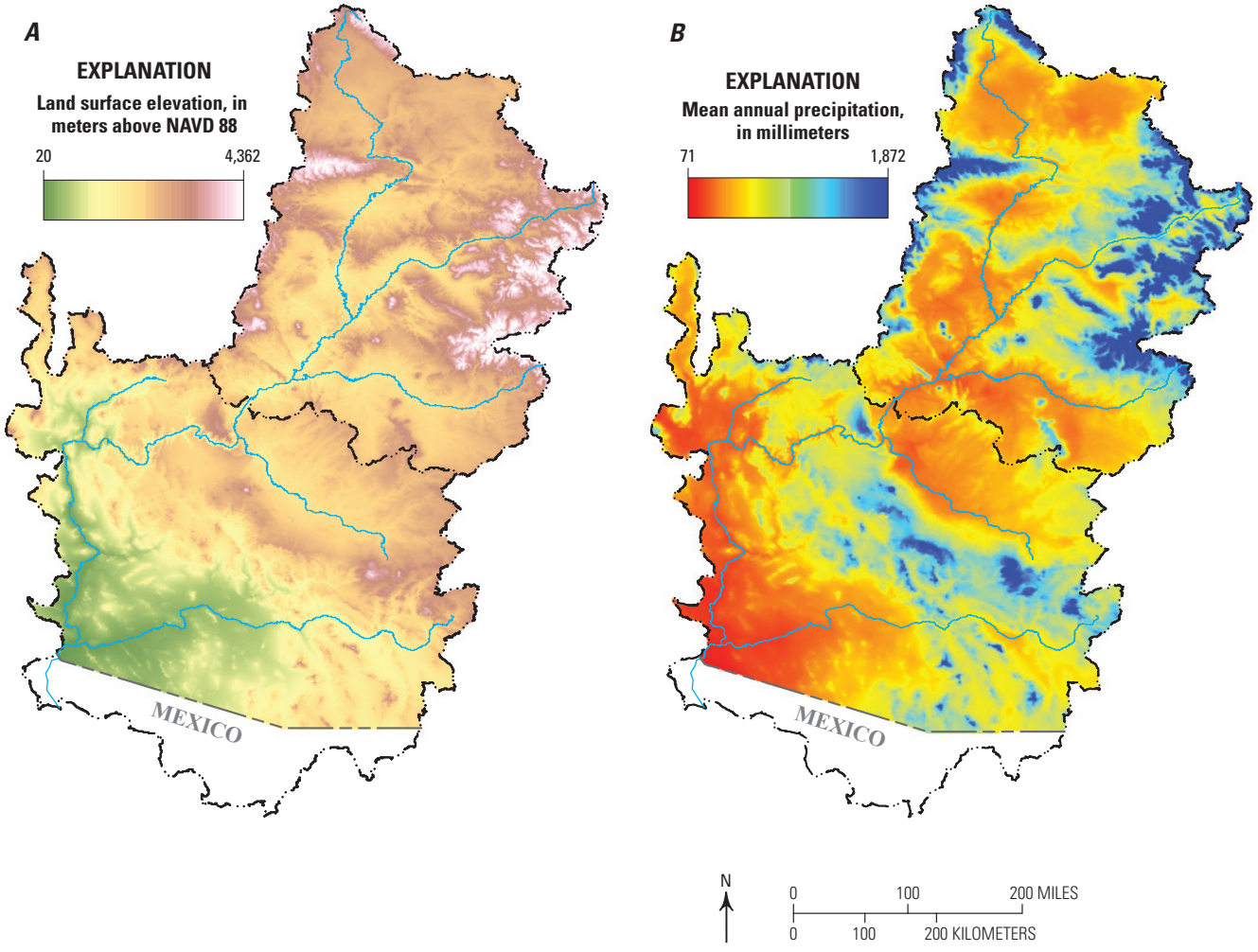

Figure 2 (pages 4–5). Maps of the Colorado River Basin (within the United States) showing: (*A*) land surface elevation above the North American Vertical Datum of 1988 (NAVD 88), (*B*) mean annual precipitation (1981–2010), and (*C*) mean annual temperature (1981–2010; PRISM Climate Group, 2019). Elevation data from the U.S. Geological Survey, National Geospatial Program.

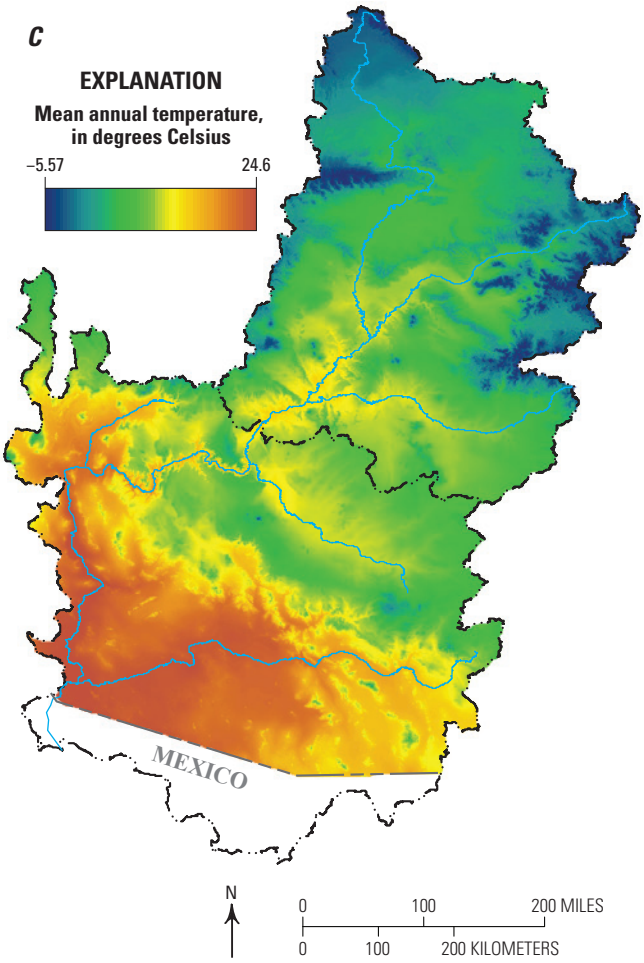

Figure 2 (pages 4–5). —Continued

hydraulic connection between aquifers in Mesozoic- and Paleozoic-age formations throughout much of the upper Colorado River Basin (Freethey and Cordy, 1991; Geldon 2003a,b). Areas with Mesozoic-age sandstone in contact with Paleozoic-age rocks and fractures associated with uplifted areas, however, may allow groundwater flow between the two systems (Geldon, 2003b). The principal aquifers in the lower basin are the basin-fill aquifers in the central and southern part of the basin (fig. 1; Robson and Banta, 1995). The basin-fill aquifers consist of unconsolidated gravel, sand, silt, and clay, or partially consolidated sedimentary or volcanic material (Robson and Banta, 1995). Structural deformations beginning in Tertiary time produced block faulting along steeply dipping normal faults. Downthrown parts of the blocks became basins and the upthrown parts became mountain ranges that mostly surround the basins. Basins were filled over time with erosional material from the mountains. Although not a principal aquifer system, the C and Redwall-Muav aquifers in northern Arizona provide important sources of water to communities on and near the Coconino Plateau (Bills and others, 2007). Permeable units of the C aquifer are contained in the Permian-age Kaibab Formation and Coconino Sandstone, and in the Esplanade Sandstone, which is the uppermost formation of the Permian- and Pennsylvanian-age Supai Group. The Redwall-Muav aquifer is named for the Mississippian-age Redwall Limestone and the Cambrian-age Muav Formation that make up the top and bottom units of the aquifer system, respectively.

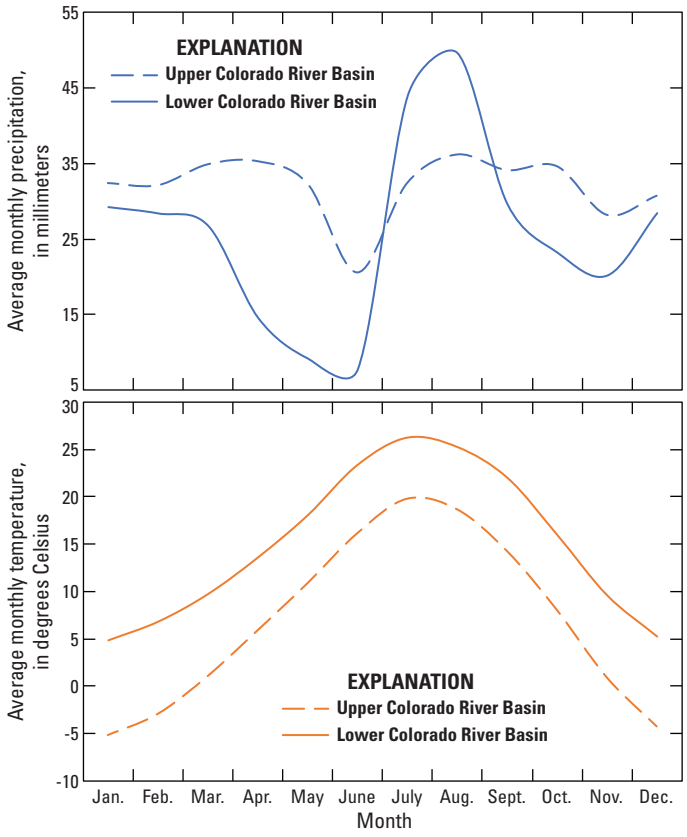

Figure 3. Graphs showing average monthly precipitation (top) and average monthly temperature (bottom) in the upper and lower Colorado River Basins during the 1896–2019 period (PRISM Climate Group, 2019).

Data and Methods

In order to understand the fundamental drivers of potential changes in groundwater recharge, first the climate parameters of precipitation and temperature are evaluated in both recent historical and projected future periods. Simulating groundwater infiltration using a numerical model is useful but adds additional uncertainty through questions about how one model might perform differently than another, how appropriate a particular model may be for a study area, or how model parameters are selected. By investigating changes in the basic climate parameters of precipitation and temperature that may increase or decrease the amount of available water for groundwater recharge, more direct information can be gained about the potential for changes in groundwater recharge that do not require numerical modeling. Recent historical climate

data are investigated to determine if conditions that affect groundwater recharge have already begun to change. Projected climate data are investigated for current understanding of possible future conditions relevant to groundwater recharge. After analyzing historical and projected temperature changes in the study area, simulations using a numerical groundwater infiltration model provide additional evidence for outcomes suggested by the climate data.

Historical climate parameters of precipitation and mean monthly temperature for the Colorado River Basin study area were evaluated using the Gridded 5km Global Historical Climatology Network (GHCN)-Daily Temperature and Precipitation Dataset (nClimGrid; Vose and others 2014a,b). The nClimGrid dataset uses station data from the GHCN with temperature bias correction and climatologically aided interpolation to address topographic and network variability, resulting in a dataset appropriate for evaluating regional climate trends (Vose and others, 2014a,b). Monthly gridded climate data, developed from the daily dataset, at approximately (~) 5-km spatial scale were available from water year (October–September) 1896 through 2019. Water year results (sum of precipitation, mean of temperature) are presented, but analyses of trends are performed on 10-year moving averages of the water year results. A 10-year averaging period is used in this study to smooth out inter-annual variability and is the averaging time used in the Colorado River compact (that is, 10-year average deliveries).

Simulated future precipitation and temperature data for the study area were available through the year 2099 for 97 climate projections from the Coupled Model Intercomparison Project phase 5 (CMIP5) multimodel archive (table 1). Each of the 97 ensemble members are results from a general climate model (GCM) run using a specified initial condition and one of four future emission scenarios known as a Representative Concentration Pathway (RCP). The four emission scenarios are for radiative forcing levels of 8.5, 6, 4.5, and 2.6 watts per square meter (W/m^2) by the end of the century (Van Vuuren, 2011). RCP8.5 represents a high baseline emission scenario that presumes "business as usual" conditions prevail. RCP2.6 represents a rapid decrease in carbon emissions in the early part of this century with a subsequent stabilization of atmospheric CO_2 concentrations by mid-century. Two medium stabilization scenarios (RCP4.5 and RCP6) represent future emissions between these end members (Van Vuuren, 2011). In this investigation, the range of future emission scenarios are all considered equally likely. GCMs are typically run at coarse spatial resolutions of ~100–200 km so climate output must be downscaled to finer spatial scales for climate effect assessments. There is a continuum of downscaling methods ranging from statistical approaches to physically based modeling. This study uses the statistical downscaling Bias-Correction and Spatial Disaggregation method (BCSD; Wood and others, 2004) to develop monthly precipitation and temperature fields at 1/8° × 1/8° (latitude × longitude) spatial resolution from the GCM native scales to be consistent with earlier analyses conducted for the upper Colorado River Basin (Tillman and others, 2016), though other statistically downscaled CMIP5 projections (for example, using the Localized Constructed Analog [LOCA]; Pierce and others, 2014, 2015) are also currently available. Little difference is observed in the study area between downscaled climate data using the BCSD and LOCA methods (Bracken, 2016).

A historical resampling and scaling technique (Wood and others, 2002) was subsequently used to disaggregate the monthly precipitation and temperature data to daily values. Projected daily precipitation and temperature data are available from the downscaled climate and hydrology projections archive hosted by Lawrence Livermore National Laboratory (Bureau of Reclamation, 2013b; https://gdo-dcp.ucllnl.org/downscaled_cmip_projections/dcpInterface.html). Summarized projected climate results for the study area discussed in this manuscript are available on the USGS ScienceBase web site (Tillman, 2017; Tillman and others, 2019).

To investigate the integrated effects of projected temperature and precipitation on groundwater resources in the study area, projected climate data from the 97 CMIP5 ensemble members were used in the Soil-Water Balance (SWB) groundwater infiltration model (Westenbroek and others, 2018). The SWB model estimates potential groundwater infiltration by calculating water-balance components using a modified version of the Thornthwaite-Mather (Thornthwaite, 1948; Thornthwaite and Mather, 1957) soil-water-balance approach (see Appendix 1 for model details and limitations). Groundwater infiltration is calculated on a daily time step as the difference between sources and sinks of water and change in soil moisture:

$$\text{INFILTRATION} = \text{water sources} - \text{water sinks} - \Delta\,\text{soil moisture} \quad (1)$$

where

water sources = rainfall + snowmelt + inflow; and
water sinks = interception + outflow + AET.

Sources of water in the SWB model include rainfall, snowmelt, and inflow from other model cells and sinks of water include interception, outflow to other model cells, and actual evapotranspiration (AET). The SWB groundwater infiltration model has been used in several regional groundwater studies in the United States including the High Plains aquifer (Stanton and others, 2011), the Lake Michigan Basin (Feinstein and others, 2010), basins in Wisconsin (Dripps and Bradbury, 2009) and Minnesota (Smith and Westenbroek, 2015), the Northern Atlantic Coastal Plain aquifer system (Masterson and others, 2013), and the upper Colorado River Basin (Tillman and others, 2016). Summarized SWB model results discussed in this manuscript are available on the USGS ScienceBase web site (Tillman, 2017; Tillman and others, 2019).

Results of both projected climate data and simulated groundwater infiltration were aggregated into water years and then subsequently averaged over 10-year periods, moving every year. The 10-year moving average smooths out inter-annual variability and makes trends more apparent. Median values for the 97 climate projections and simulated

Table 1. Institutions providing climate model output used in the Colorado River Basin climate and groundwater infiltration investigation.

[Abbreviations: BCC, Beijing Climate Center, China Meteorological Administration; CCCMA, Canadian Centre for Climate Modelling and Analysis; CMCC, Centro Euro-Mediterraneo per I Cambiamenti Climatici; CNRM-CERFACS, Centre National de Recherches Météorologiques /Centre Européen de Recherche et Formation Avancée en Calcul Scientifique; CSIRO-BOM, Commonwealth Scientific and Industrial Research Organization (CSIRO) and Bureau of Meteorology (BOM), Australia; CSIRO-QCCCE, Commonwealth Scientific and Industrial Research Organization in collaboration with Queensland Climate Change Centre of Excellence; FIO, The First Institute of Oceanography, State Oceanic Administration, China; INM, Institute for Numerical Mathematics; IPSL, Institut Pierre-Simon Laplace; LASG-CESS, LASG, Institute of Atmospheric Physics, Chinese Academy of Sciences and CESS,Tsinghua University; MIROC, Atmosphere and Ocean Research Institute (The University of Tokyo), National Institute for Environmental Studies, and Japan Agency for Marine-Earth Science and Technology; MIROC(2), Japan Agency for Marine-Earth Science and Technology, Atmosphere and Ocean Research Institute (The University of Tokyo), and National Institute for Environmental Studies; MOHC, Met Office Hadley Centre (additional HadGEM2-ES realizations contributed by Instituto Nacional de Pesquisas Espaciais); MPI-M, Max-Planck-Institut für Meteorologie (Max Planck Institute for Meteorology); MRI, Meteorological Research Institute; NASA GISS, National Aeronautics and Space Administration Goddard Institute for Space Studies; NCAR, National Center for Atmospheric Research; NCC, Norwegian Climate Centre; NOAA GFDL, National Oceanic and Atmospheric Administration Geophysical Fluid Dynamics Laboratory; NSF-DOE-NCAR, National Science Foundation - Department of Energy - National Center for Atmospheric Research Community Earth System Model Contributors]

Modeling Center or Group	Model Name	Representative Concentration Pathway			
		2.6	4.5	6.0	8.5
BCC	BCC-CSM 1.1	✓	✓	✓	✓
BCC	BCC-CSM 1.1(m)		✓		✓
CCCMA	CanESM2	✓	✓		✓
CMCC	CMCC-CM		✓		✓
CNRM-CERFACS	CNRM-CM5		✓		✓
CSIRO-BOM	Access 1.0		✓		✓
CSIRO-QCCCE	CSIRO-mk3.6.0	✓	✓	✓	✓
FIO	FIO-ESM	✓	✓	✓	✓
INM	INM-CM4		✓		✓
IPSL	IPSL-CM5A-MR	✓	✓	✓	✓
IPSL	IPSL-CM5B-LR		✓		✓
LASG-CESS	FGOALS-g2	✓	✓		✓
MIROC	MIROC5	✓	✓	✓	✓
MIROC(2)	MIROC-ESM	✓	✓	✓	✓
MIROC(2)	MIROC-ESM-CHEM	✓	✓	✓	✓
MOHC	HadGEM2-AO	✓	✓	✓	✓
MOHC	HadGEM2-CC		✓		✓
MOHC	HadGEM2-ES	✓	✓	✓	✓
MPI-M	MPI-ESM-LR	✓	✓		✓
MPI-M	MPI-ESM-MR	✓	✓		✓
MRI	MRI-CGCM3	✓	✓		✓
NASA GISS	GISS-E2-H-CC		✓		
NASA GISS	GISS-E2-R	✓	✓	✓	✓
NASA GISS	GISS-E2-R-CC		✓		
NCAR	CCSM4(RSMAS)	✓	✓	✓	✓
NCC	NorESM1-M	✓	✓	✓	✓
NOAA GFDL	GFDL-CM3	✓	✓	✓	✓
NOAA GFDL	GFDL-ESM2G	✓	✓	✓	✓
NOAA GFDL	GFDL-ESM2M	✓	✓	✓	✓
NSF-DOE-NCAR	CESM1(BGC)		✓		✓
NSF-DOE-NCAR	CESM1(CAM5)	✓	✓	✓	✓

groundwater infiltration are used to describe the central tendency (50th percentile) of the projected climate and infiltration results, with the interquartile range (25th and 75th percentiles) of results presented to illustrate variability in the projected data and model results. Results for projected climate data and simulated groundwater infiltration are presented as a percentage of the recent historical (water years 1951–2015) average. For projected temperature results, both mean temperature and potential evapotranspiration (PET) are discussed. The Hargreaves-Samani (Hargreaves and Samani, 1985) estimation of PET, which is used in this study in the estimation of actual evapotranspiration (AET) in equation 1, is directly related to temperature and is more easily compared on a seasonal scale (for example, percent contribution from a season to a year) than temperature. Projected climate and SWB simulation analyses for the upper Colorado River Basin in this study are based on previously published results (Tillman and others, 2016).

Descriptive, correlative, and hypothesis-testing statistics were performed using the R statistical platform, version 3.6.0 (R Core Team, 2019). A significant statistical test result was defined as having a p-value<0.05.

Analyses of Recent Historical Climate Data for the Colorado River Basin

Historical precipitation and temperature data for the study area were available from water year 1896 through 2019. Patterns are difficult to observe in individual water-year values, but 10-year moving averages illustrate 10-to 20-year cycles in precipitation in both the upper and lower basins (fig. 4). Ten-year moving averages of precipitation show more variability in the lower basin (variance is 778 square millimeters [mm^2]) than the upper basin (variance is 315 mm^2). Relative to the long-term (1896–2019) average,

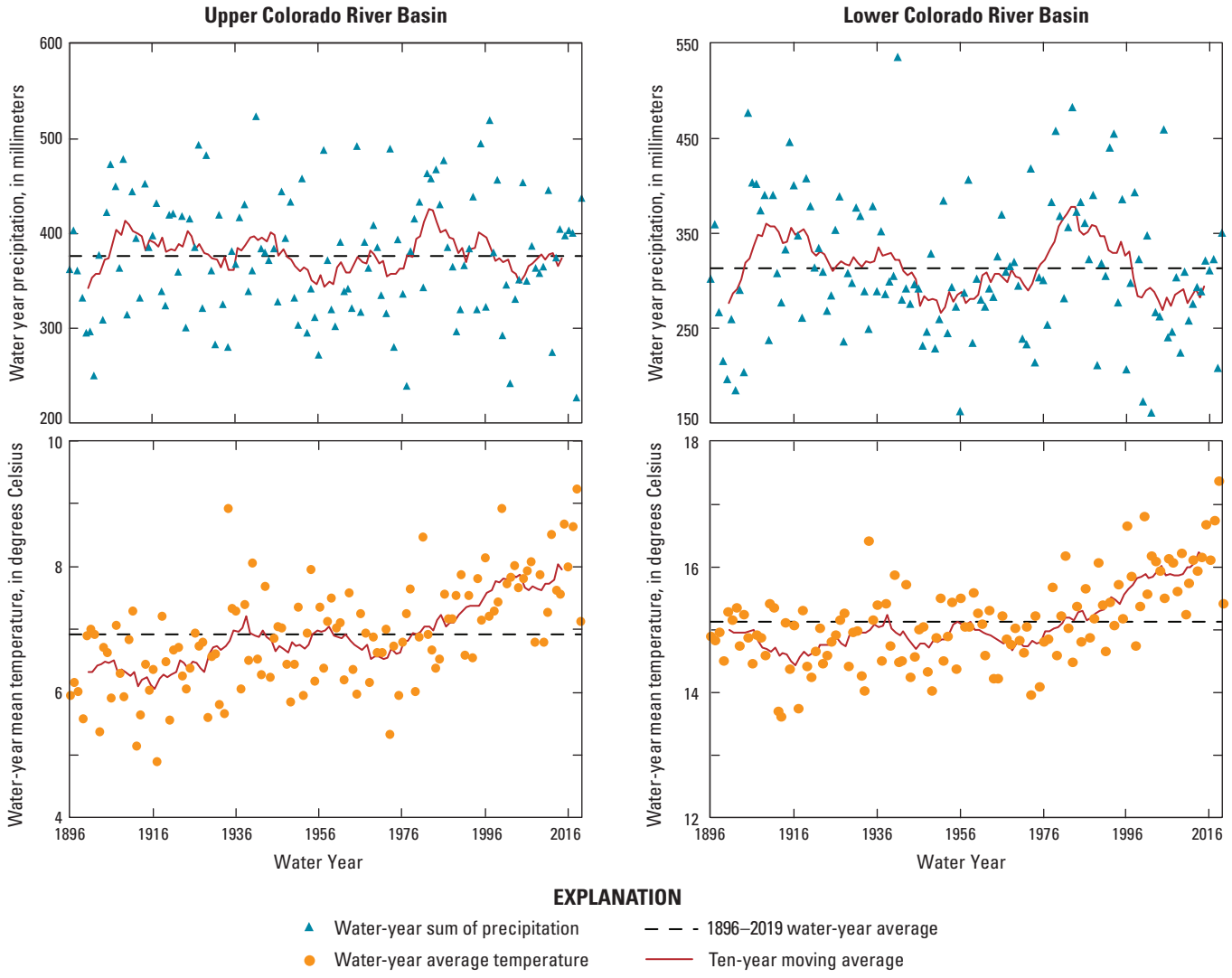

Figure 4. Graphs showing historical precipitation (top plots) and temperature (bottom plots) in the upper and lower Colorado River Basins during the 1896–2019 period (Vose and others, 2014a,b). Note different vertical scales for the two basins.

the maximum wet period for the upper basin is the decade 1978–1987 (13 percent above the mean) and the decade 1979–1988 (21 percent above the mean) for the lower basin. The maximum dry periods during the recent historical record are 1896–1905 for the upper basin (9 percent below average) and 1946–1955 for the lower basin (15 percent below average). More recently, 10-year moving averages of precipitation have been mostly below the long-term (1896–2019) average. Beginning with the 1993–2002 10-year period, 78 percent of upper basin and 100 percent of the lower basin decades have experienced precipitation less than the 1896–2019 average (fig. 4). Although upper basin precipitation data indicate no statistical trend (p-value>0.05) over the 1896–2019 historical period, the lower basin has a weak negative trend over this period (Kendall's τ =−0.2, p-value=0.001).

Multidecadal-scale cyclical patterns in temperature also are observed in historical climate data in both the upper and lower basins, at least until the early 1970s (fig. 4). The coolest period for both the upper and lower basins was the 1912–1921 decade, when temperatures were 0.86 °C (12 percent) and 0.70 °C (5 percent) below historical means, respectively. Prior to the early 1970s, the warmest period for both the upper and lower basins was the 1934–1943 decade, when temperatures were 0.3 °C (4 percent) and 0.1 °C (0.6 percent) above their respective long-term means. Beginning in the early 1970s, both the upper basin (Kendall's τ=0.83, p-value<2.5×10^{-15}) and lower basin (Kendall's τ=0.91, p-value<2.2×10^{-16}) experienced strong, monotonic positive trends in temperature, with a maximum rise above long-term means to date of 1.1 °C for both basins.

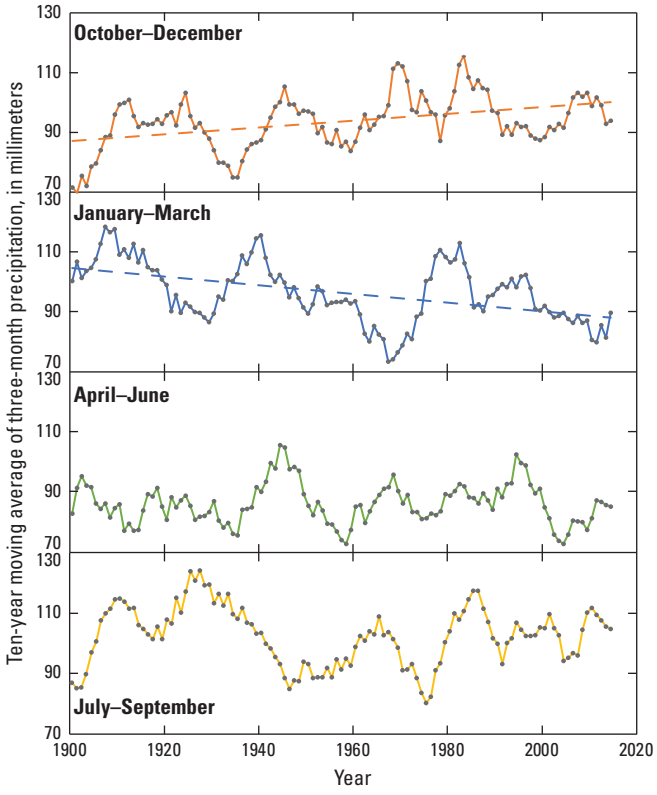

Figure 5. Graphs showing precipitation over three-month periods in the upper Colorado River Basin during the 1896–2019 period (Vose and others, 2014a,b). Dashed line indicates significant slope of linear regression and significant correlation with time (p-value<0.05).

Seasonal precipitation in the upper basin over the recent historical period (fig. 5) is characterized by significantly increasing precipitation in the October–December months (Kendall's τ=0.25, p-value=7.9×10^{-5}) and significantly decreasing precipitation in the January–March months (Kendall's τ=−0.36, p-value=9.7×10^{-9}). Lower basin seasonal precipitation (fig. 6) decreased in the historical period in April–June (Kendall's τ=−0.36, p-value=8.2×10^{-9}) and July–September (Kendall's τ =−0.22, p-value =4.1×10^{-4}) months. Significant positive trends in temperature are observed in the recent historical period across all seasons for both the upper (fig. 7) and lower (fig. 8) basins, with greatest increases in July–September for the upper basin (Kendall's τ=0.61, p-value<2.2×10^{-16}) and in October–December for the lower basin (Kendall's τ=0.54, p-value<2.2×10^{-16}).

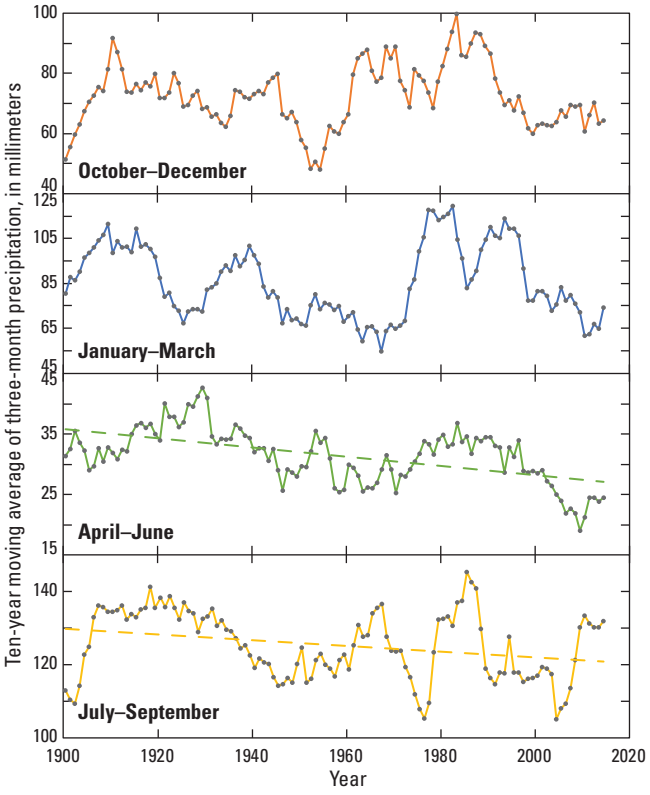

Figure 6. Graphs showing precipitation over three-month periods in the lower Colorado River Basin during the 1896–2019 period (Vose and others, 2014a,b). Dashed line indicates significant slope of linear regression and significant correlation with time (p-value<0.05).

Possible effects of observed trends in climate data on groundwater resources can be discussed conceptually by evaluating a simple water balance equation for groundwater infiltration, such as equation 1. No trend in decadal

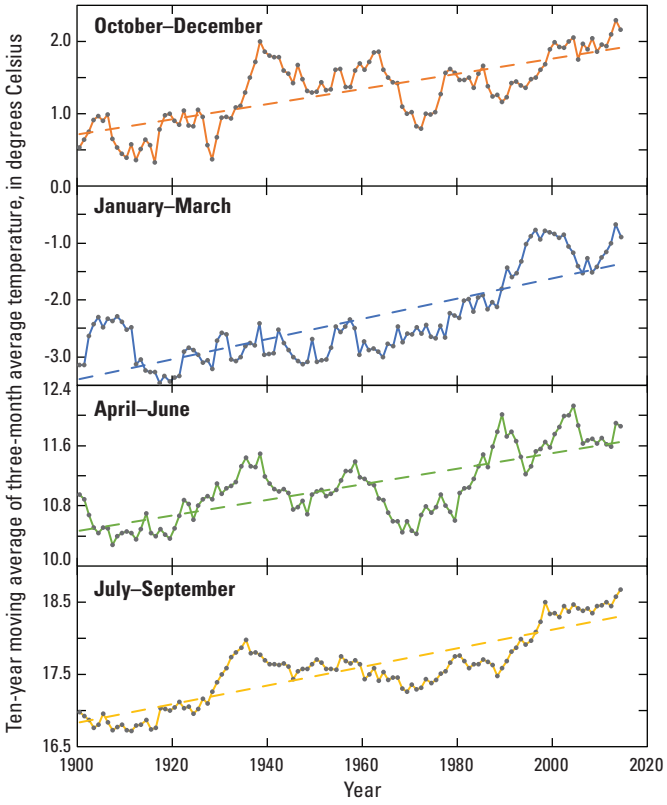

Figure 7. Graphs showing average temperature over three-month periods in the upper Colorado River Basin during the 1896–2019 period (Vose and others, 2014a,b). Dashed line indicates significant slope of linear regression and significant correlation with time (*p*-value<0.05).

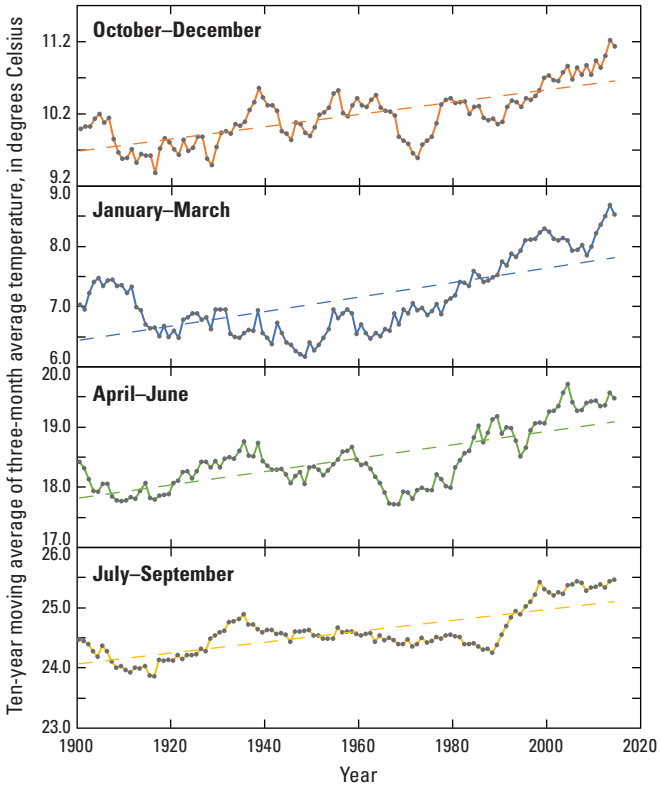

Figure 8. Graphs showing average temperature over three-month periods in the lower Colorado River Basin during the 1896–2019 period (Vose and others, 2014a,b). Dashed line indicates significant slope of linear regression and significant correlation with time (*p*-value<0.05).

precipitation in the upper basin means little change in the longer term "water sources" part of equation 1. The negative trend in decadal precipitation in the lower basin would result in less groundwater infiltration over time, all other conditions being the same in equation 1. However, other terms in equation 1 are not the same over the recent historical period. Temperature increases in both the upper and lower basins since the early 1970s would increase evapotranspiration rates, increasing the "water sinks" part of equation 1, resulting in a decrease in water available for groundwater infiltration. This increase in water removed from the system permanently would compound the possible reduction in groundwater infiltration caused solely by the decrease in precipitation noted in lower basin climate records (Cook and others, 2015). Significantly decreasing precipitation in the January–March months observed in the upper basin may further decrease groundwater infiltration above estimates using annual precipitation values, as spring snowmelt is a principal source of water for groundwater infiltration in the upper basin (Earman and others, 2006; Whitehead, 1996).

Analyses of Projected Climate Data for the Colorado River Basin

GCM precipitation and temperature data for the study area were available from water years 1951 through 2099. Median and interquartile ranges of 10-year moving averages of 97 CMIP5 climate model projections are presented relative to results from the recent historical period (1951–2015). In the upper basin (fig. 9*A*), precipitation is expected to increase throughout the projected future period. By mid-century, median projected decadal precipitation is expected to be about 6 percent greater than the recent historical period (1951–2015). By the end of the century, projected precipitation rises to 9 percent above the 1951–2015 period. Most of the 97 climate projections concur with the projected increase in precipitation, with even the 25th percentile of results barely below, and during a few periods above, the historical median. The relative seasonal contribution of precipitation in a water year (fig. 9*B*) is not projected to change over time, with about one-quarter of

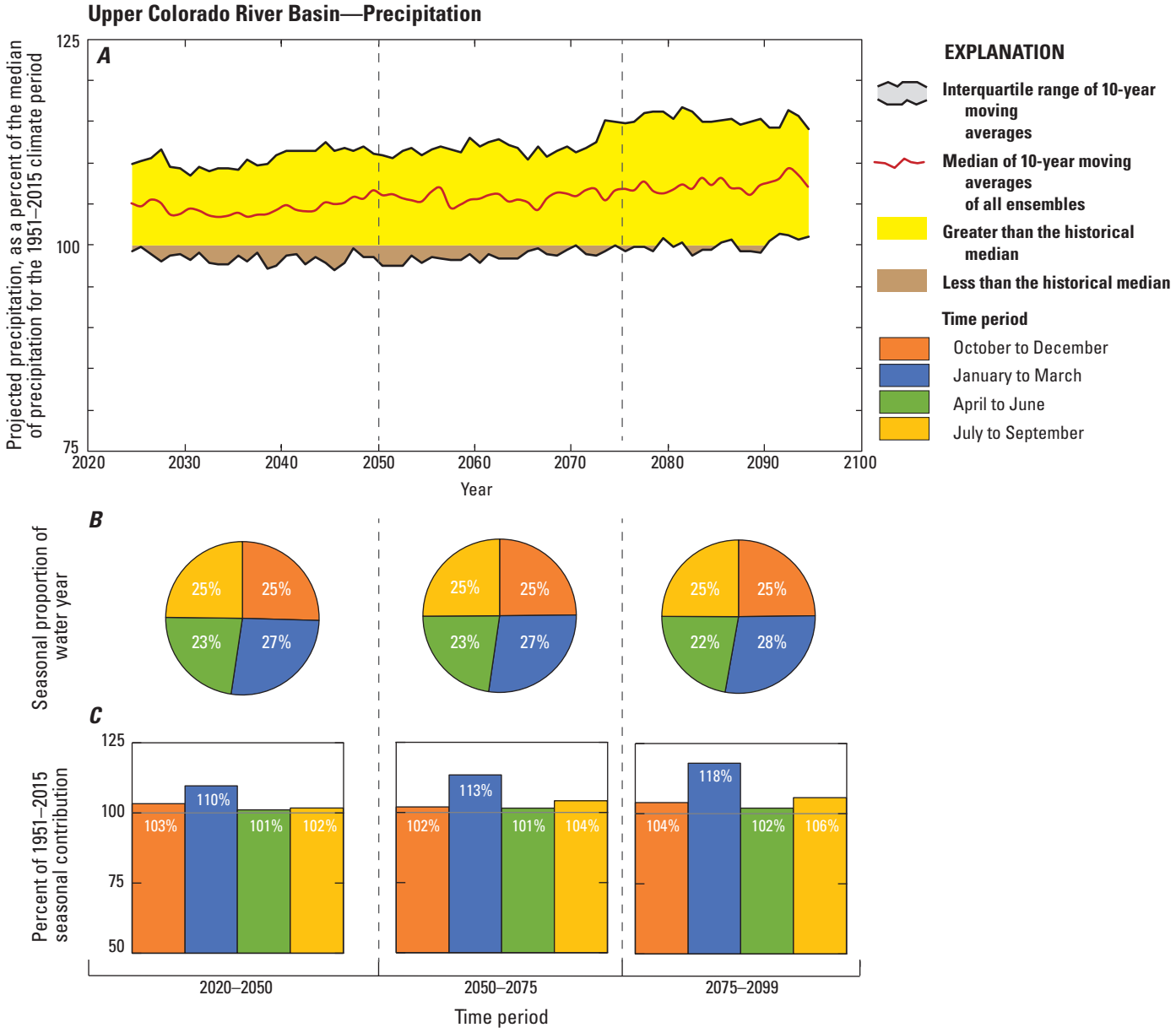

Figure 9. Diagrams and graphs showing median and interquartile range of 10-year moving averages of projected precipitation (*A*), proportional seasonal contribution to water-year precipitation (*B*), and change in seasonal precipitation relative to 1951–2015 precipitation (*C*) for the upper Colorado River Basin. Pie diagrams and bar graphs summarize results over decades 2020–29 to 2045–54, 2046–55 to 2070–79, and 2071–80 to 2090–99. Line graph in *A* adapted from Tillman and others (2016) , used with permission. %, percent.

precipitation projected in each 3-month period throughout the century. Seasonal contributions relative to the historical period (fig. 9*C*), however, indicate that most of the projected increase in precipitation is in January–March, during which cooler temperatures may provide favorable conditions for increased groundwater infiltration. The projected substantial increase in January–March precipitation, however, is not supported by trends in recent historical data (fig. 5).

Temperature in the upper basin also is projected to be above the recent historical median throughout the rest of the century, with steady warming in decadal average temperatures expected until the last quarter of this century, when projected temperature levels out (fig. 10*A*). The climate models are in even greater agreement about projected warming temperatures than projected increases in precipitation, as evidenced by a narrower interquartile range and the 25th percentile of

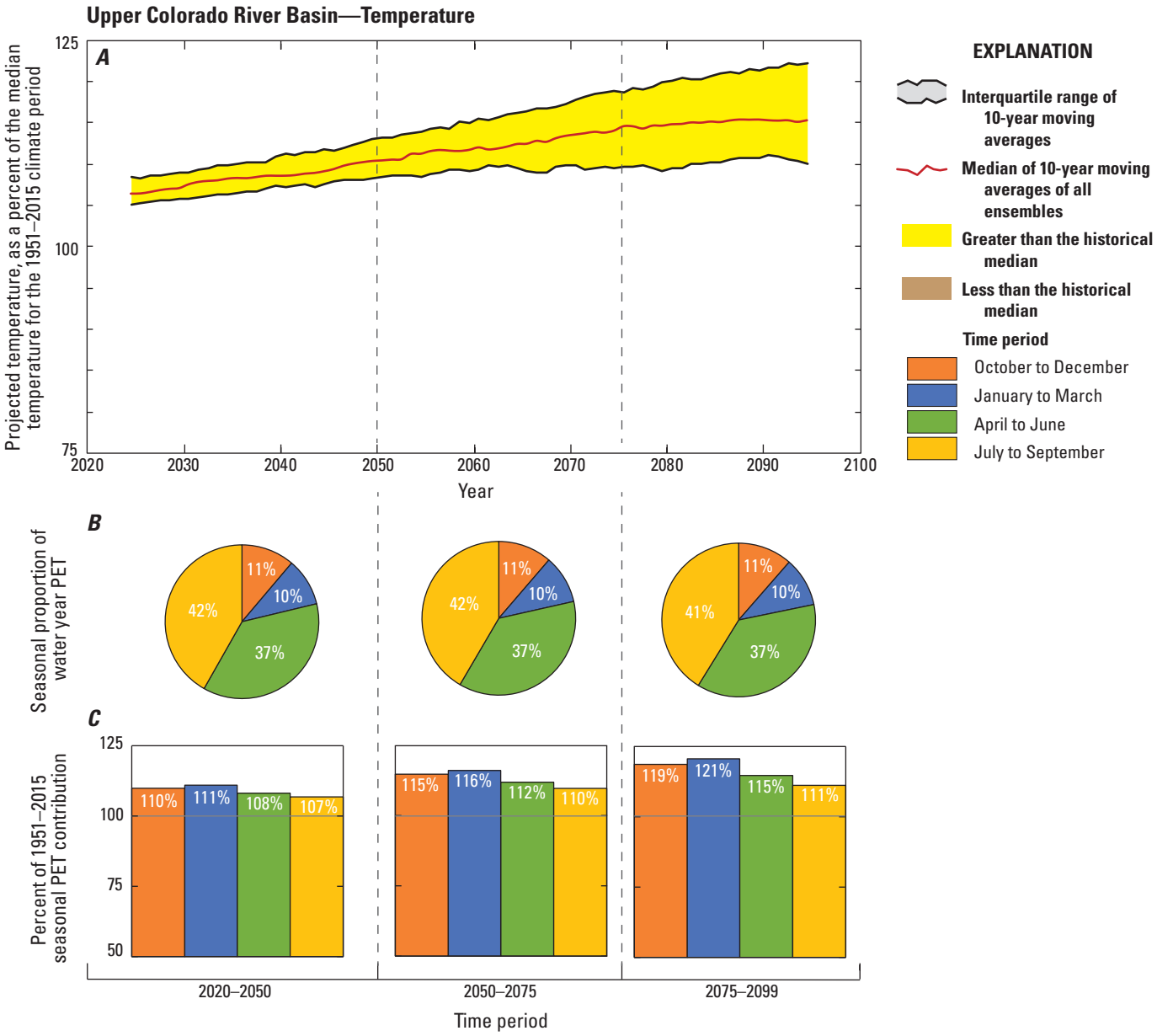

Figure 10. Diagrams and graphs showing median and interquartile range of 10-year moving averages of projected temperature (*A*), proportional seasonal contribution to water-year potential evapotranspiration (PET) (*B*), and change in seasonal PET relative to 1951–2015 PET (*C*) for the upper Colorado River Basin. Pie diagrams and bar graphs summarize results over decades 2020–29 to 2045–54, 2046–55 to 2070–79, and 2071–80 to 2090–99. Line graph in A modified from Tillman and others (2016), used with permission. %, percent.

ensembles warmer than the historical median throughout all decades of the century. Relative seasonal contributions of projected increased temperature, as demonstrated by analyses of potential evapotranspiration (PET) in fig. 10*B*, remain constant throughout the century. Lowest seasonal PET is projected to remain during the cooler months of January–March, although this season is projected to have the greatest increase in temperature (fig. 10*C*). The increase in temperature during January–March may negate the effect on increased water available for groundwater infiltration that would be expected from the projected increase in precipitation during the same months (fig. 9). Projected warming throughout all seasons is supported by positive trends in temperature in recent historical data (fig. 7).

In contrast to projected precipitation in the upper basin (fig. 9), precipitation in the lower basin is projected to be the same as, or slightly (<3 percent) less than, the historical period throughout most of the rest of this century (fig. 11*A*).

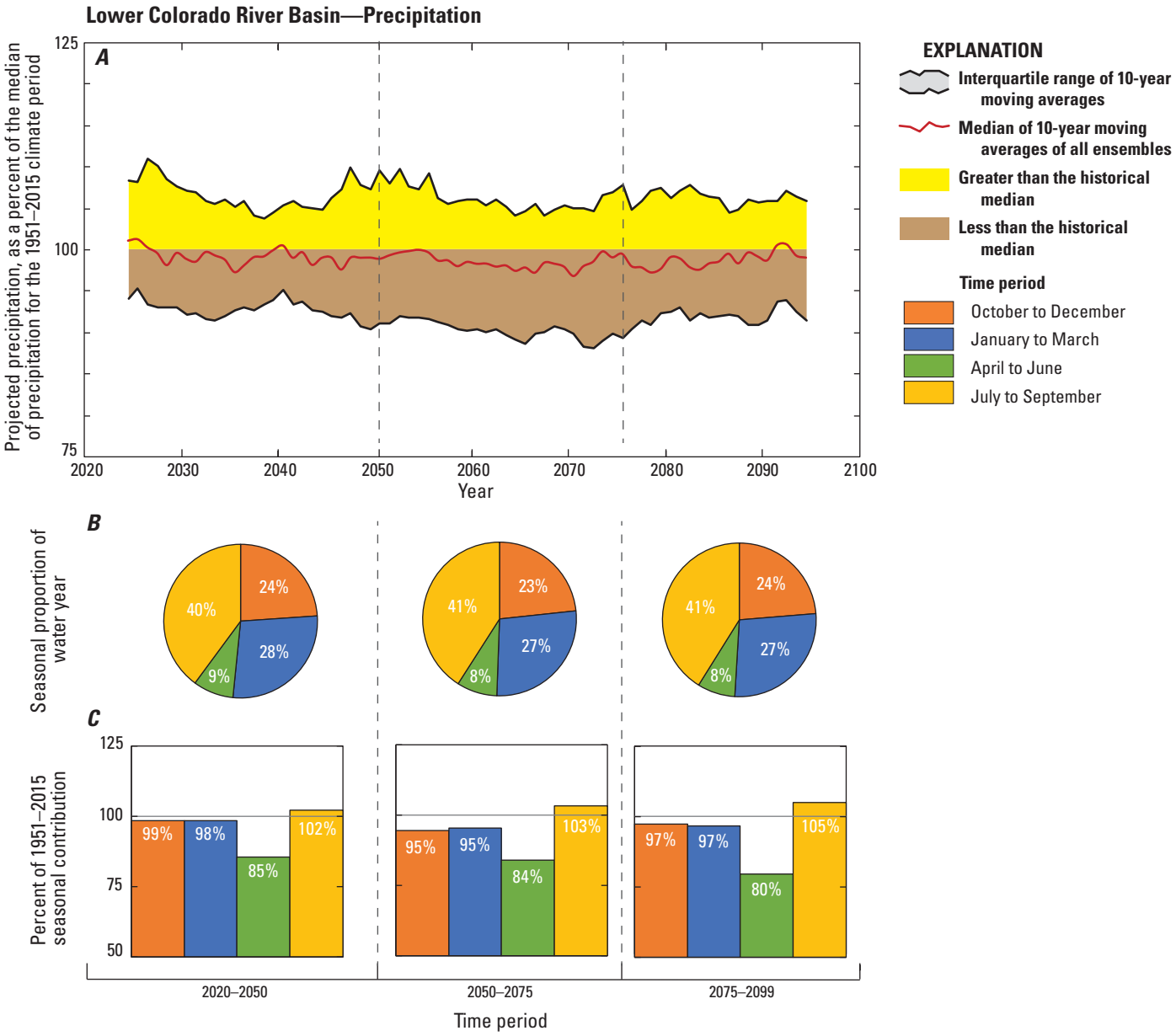

Figure 11. Diagrams and graphs showing median and interquartile range of 10-year moving averages of projected precipitation (*A*), proportional seasonal contribution to water-year precipitation (*B*), and change in seasonal precipitation relative to 1951–2015 precipitation (*C*) for the lower Colorado River Basin. Pie diagrams and bar graphs summarize results over decades 2020–29 to 2045–54, 2046–55 to 2070–79, and 2071–80 to 2090–99.%, percent.

This conclusion is based on the median of the 97 climate ensembles, but variability in climate projections demonstrated by the interquartile range of results indicates precipitation could be slightly above or below the historical period. As with the upper basin, the interquartile range of projected precipitation in the lower basin is substantially wider than for projected temperature, indicating a lack of certainty among climate model-projected precipitation that has been documented in other studies (Schaller and others, 2011). The relative seasonal contribution of precipitation in a water year (fig. 11*B*), is projected to remain mostly the same throughout the century, with a slight decrease in the water-year proportion of precipitation during April–June and a slight increase in relative July–September precipitation over time. For the seasonal periods with the greatest contribution to water-year precipitation, October–December and January–March are projected to be slightly (<3 percent) less than during the historical period (fig. 11*C*) , whereas July–September

precipitation is projected to be slightly greater (maximum of 5 percent) than during the historical period. Projected increase in July–September precipitation is unlikely to benefit groundwater systems in much of the lower basin, however, as high temperatures and resulting PET rates during this season would likely limit additional available water for groundwater infiltration. Projected decreases in April–June months are supported by negative trends in historical precipitation data (fig. 6). Projected increase in July–September precipitation contrasts with a negative trend in these months during the recent historical period (fig. 6).

Like projected temperature in the upper basin, temperature in the lower basin also is projected to be above the recent historical median throughout the rest of the century (fig. 12*A*). A narrow interquartile range, and 25th percentile of ensembles for all remaining decades of the century warmer than the historical median, demonstrate consensus on this projected warming among climate models. Relative seasonal contributions of projected increased temperature, as demonstrated by analyses of potential evapotranspiration (PET) (fig. 12*B*), remain mostly constant throughout the century, with highest PET during the warmer April–June and

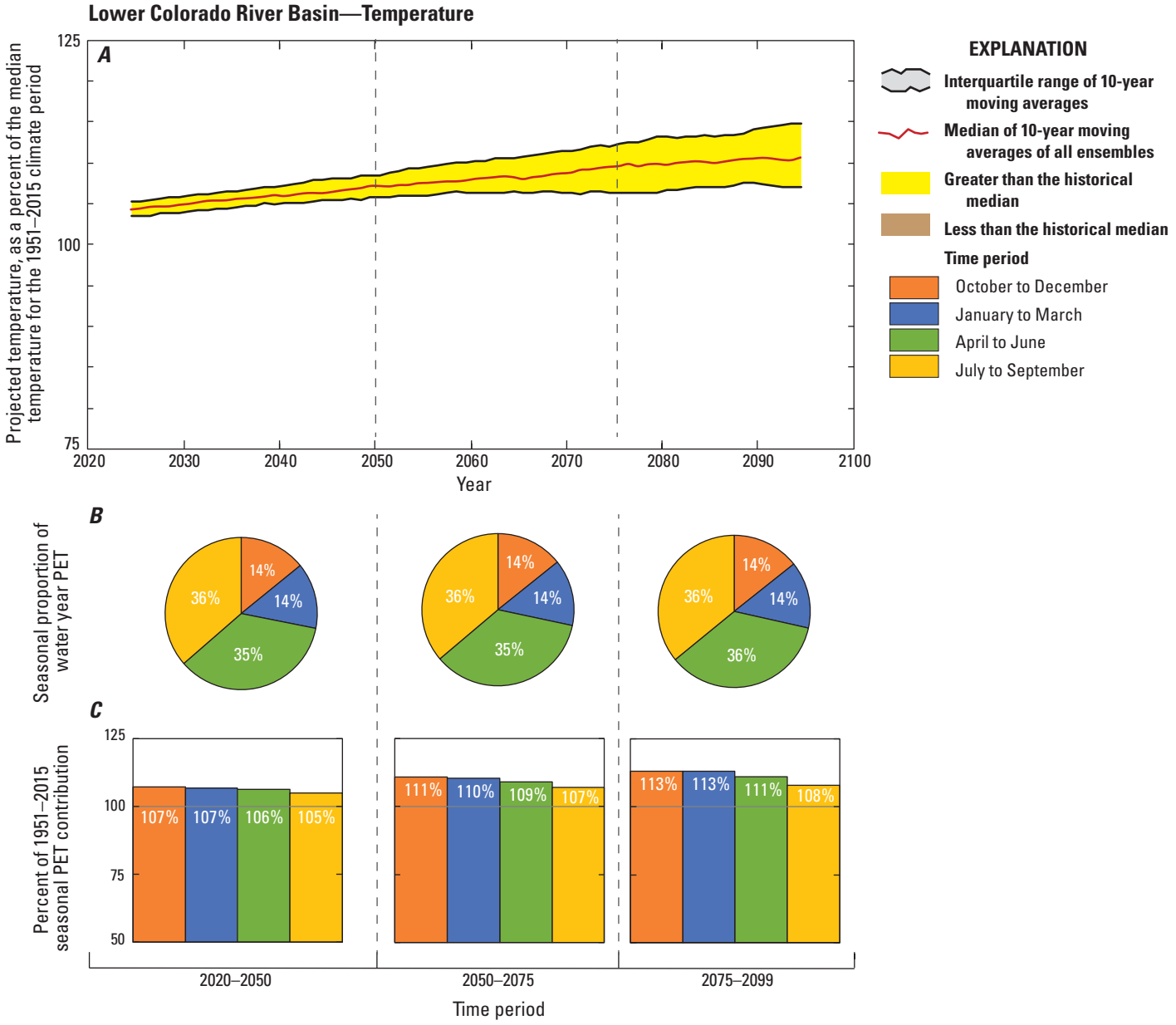

Figure 12. Diagrams and graphs showing median and interquartile range of 10-year moving averages of projected temperature (*A*), proportional seasonal contribution to water-year potential evapotranspiration (PET) (*B*), and change in seasonal PET relative to 1951–2015 PET (*C*) for the lower Colorado River Basin. Pie diagrams and bar graphs summarize results over decades 2020–29 to 2045–54, 2046–55 to 2070–79, and 2071–80 to 2090–99.%, percent.

July–September months and the lowest during the cooler October–December and January–March months. All seasonal PET is projected to increase, relative to the historical period, throughout the rest of the century (fig. 12*C*), with the greatest increase (13 percent) in both the October–December and January–March months. Increases in temperature during the cooler October–December and January–March months (fig. 12*C*) combined with projected decreases in precipitation during these same periods (fig. 11*C*) are expected to decrease the amount of available water for groundwater infiltration. Projected warming across all seasons is supported by positive trends in temperature in recent historical data (fig. 8).

Comparing median projections for all future decades with median results from all historical decades (fig. 13), future precipitation is expected to be greater than that of the past in the upper basin (Wilcoxon rank sum, p-value$<2.2\times10^{-16}$, one-tailed), though no significant difference is projected for precipitation in the lower basin (Wilcoxon rank sum, p-value = 0.999, one-tailed). Moreover, the 10th percentile of average annual precipitation in all future decades exceeds precipitation in the 90th percentile of historical decades in the upper basin. Comparing the distribution of projected and historical temperature in the Colorado River Basin, significant increases in temperature are expected in both the upper (Wilcoxon rank sum, p-value$<2.2\times10^{-16}$, one tailed) and lower (Wilcoxon rank sum, p-value$<2.2\times10^{-16}$, one tailed) basins (fig. 13).

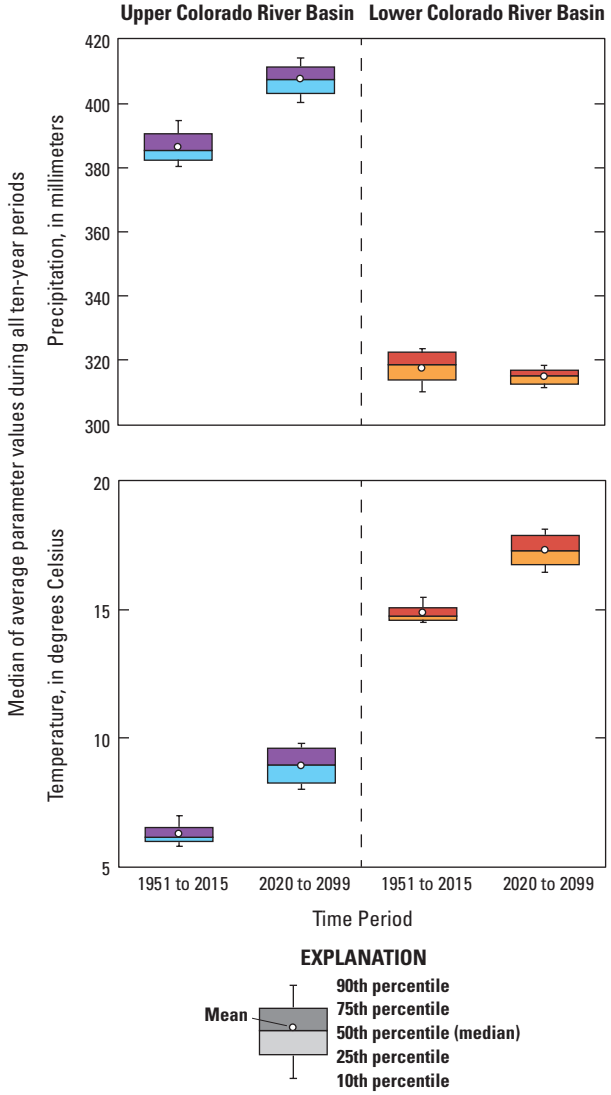

Figure 13. Boxplots comparing median decadal-average precipitation and temperature between recent historical and future periods for the upper and lower Colorado River Basins.

Projected Groundwater Infiltration for the Colorado River Basin

Projected precipitation and temperature results from the 97 CMIP5 climate projections were used to drive changes in simulated groundwater infiltration using the Soil-Water Balance model. As previously described by Tillman and others (2016), central tendency of SWB simulation results indicate that the upper Colorado River Basin is expected to experience mostly decades of above-historical-average groundwater infiltration through the end of the century (fig. 14*A*). Owing to the compounded variability of both precipitation and temperature inputs to the model, the interquartile range of simulated groundwater infiltration is relatively large. The largest proportion of water-year simulated groundwater infiltration is during the April–June months, when 65–74 percent of infiltration occurs (fig. 14*B*). The increase in January–March contribution to water-year simulated infiltration through the end of the century comes at the expense of a decrease in April–June contribution over the same period. Relative to the historical period, a large increase is projected in January–March groundwater infiltration and a decrease is projected in April–June infiltration (fig. 14*C*), the two seasons that account for about 95 percent of water-year infiltration (fig. 14*B*). Projected January–March precipitation increases over historical decades by 18 percent by the end of the century (fig. 9*C*), but large increases in PET (21 percent) also are expected during these months (fig. 10*C*). Relatively cool temperatures during the January–March months (only 10 percent of water-year PET, fig. 10*B*), however, result in much of the increase in precipitation being available for groundwater infiltration. The projected 18 percent decrease in simulated April–June groundwater infiltration relative to historical decades (fig. 14*C*) can be explained by fairly flat projected precipitation (fig. 9*C*) combined with projected increase in PET (fig. 10*C*) resulting in less water available for groundwater systems. In addition to these direct effects, precipitation that was historically stored as snow during January–March and released for infiltration during the April–June snowmelt season may be reduced by warming temperatures, resulting in increased January–March and decreased April–June simulated infiltration. Simulated infiltration during the July–September months decreases by 35 percent by the end of the century, owing to increasing temperature (fig. 10), and simulated October–December

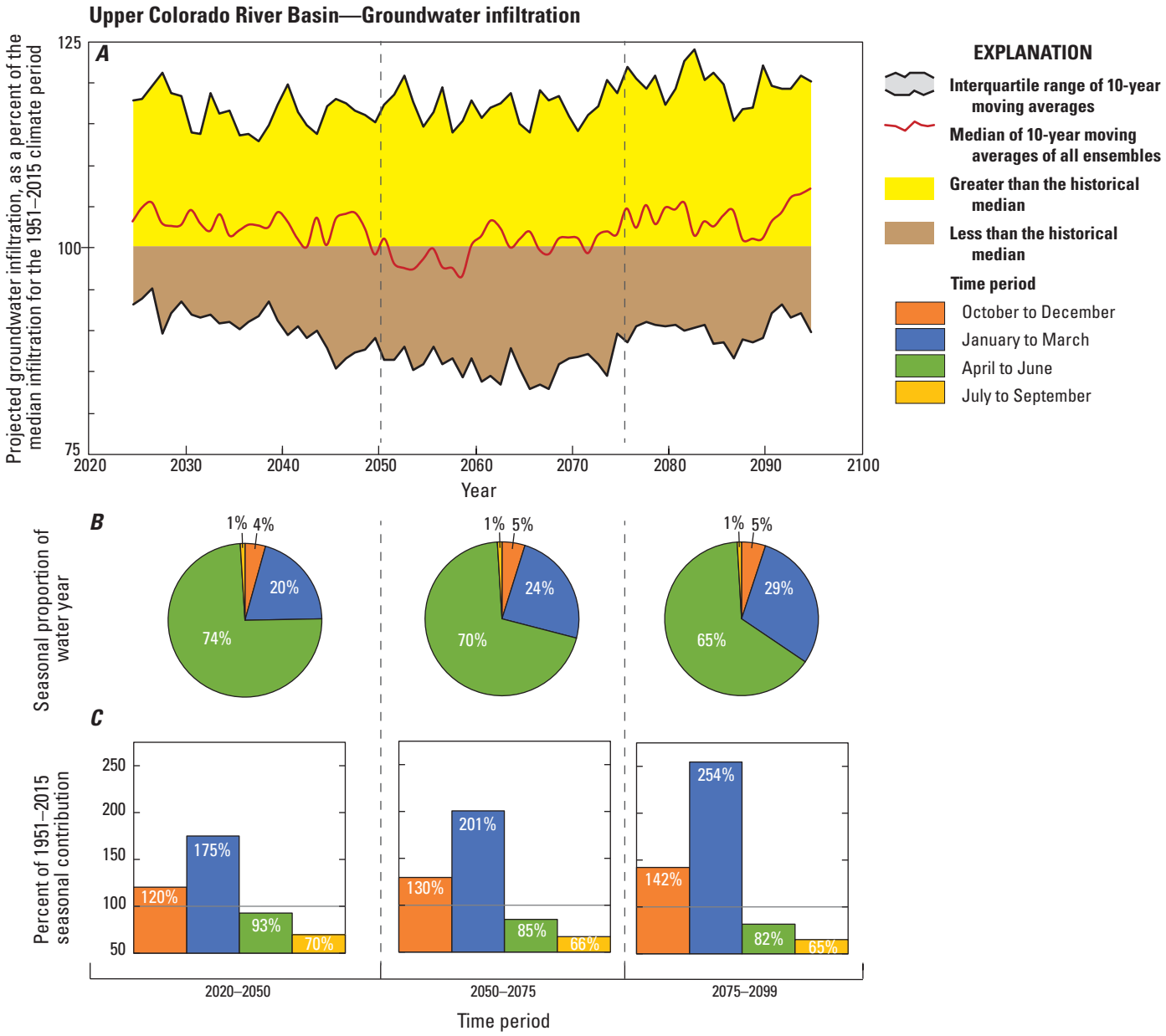

Figure 14. Diagrams and graphs showing median and interquartile range of 10-year moving averages of simulated projected groundwater infiltration (*A*), proportional seasonal contribution to water-year infiltration (*B*), and change in seasonal infiltration relative to 1951–2015 infiltration (*C*) for the upper Colorado River Basin. Pie diagrams and bar graphs summarize results decades 2020–29 to 2045–54, 2046–55 to 2070–79, and 2071–80 to 2090–99. Line graph in *A* modified from Tillman and others (2016), used with permission. %, percent.

infiltration increases by 42 percent, owing to increasing precipitation (fig. 9), although these seasons contribute only 1 percent and 5 percent to water-year infiltration, respectively (fig. 14*B*). Results from simulated groundwater infiltration indicate that projected increases in precipitation during winter months provides additional water for groundwater infiltration despite projected increases in temperature during these months. Increases in projected precipitation during warmer months of the year, however, are not enough to compensate for projected increase in PET in these water-limited months, resulting in declines in projected infiltration during these seasons.

In the lower Colorado River Basin, simulated groundwater infiltration is projected to be consistently less than the recent historical period for most of the remaining century (fig. 15). Decadal average groundwater infiltration is expected to decrease by as much as 16 percent below the recent historical period by 2059–2068. In contrast to upper basin simulated groundwater infiltration (fig. 14),

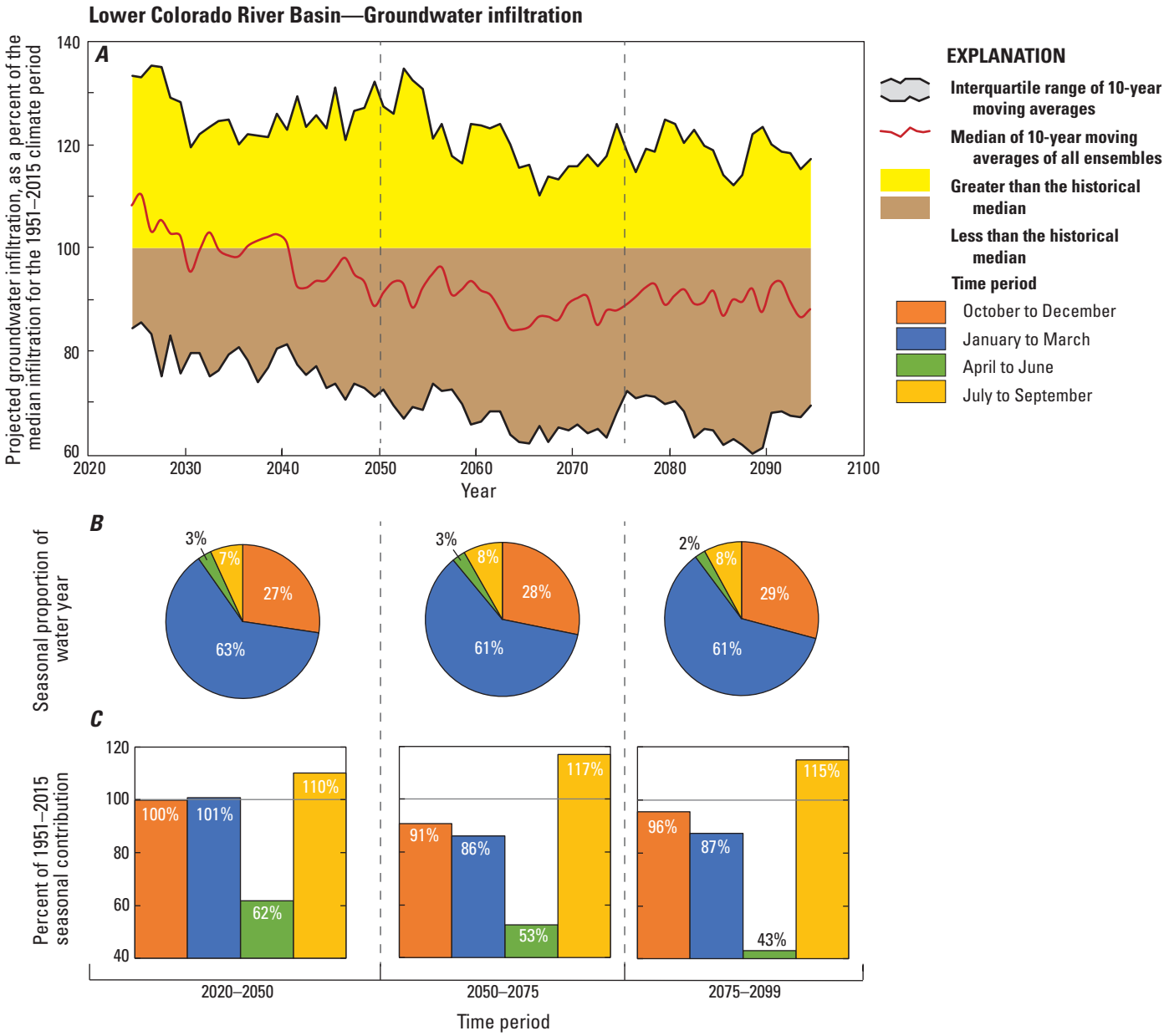

Figure 15. Diagrams and graphs showing median and interquartile range of 10-year moving averages of simulated projected groundwater infiltration (*A*), proportional seasonal contribution to water-year infiltration (B), and change in seasonal infiltration relative to 1951–2015 infiltration (*C*) for the lower Colorado River Basin. Pie diagrams and bar graphs summarize results over decades 2020–29 to 2045–54, 2046–55 to 2070–79, and 2071–80 to 2090–99.%, percent.

most water-year lower basin infiltration occurs during the January–March period (fig. 15*B*), although some decrease in this proportion is projected by the end of the century. A small decrease in projected precipitation during January–March (fig. 11*C*) combined with a substantial increase in PET (7–13 percent; fig. 12*C*) during this time is responsible for this projected decline in groundwater infiltration. Although the water-year proportion of October–December simulated groundwater infiltration is projected to increase over time (fig. 15*B*), the total amount of infiltration is projected to decrease during this season (fig. 15*C*). Similar to projected infiltration during the January–March months, the reduction in October–December infiltration is a response to a small decrease in projected precipitation (fig. 11*C*) combined with a substantial projected increase in PET (7–13 percent; fig. 12*C*) during these months. The only season projected to experience an increase in groundwater infiltration is during the July–September months (by as much as 17 percent during mid-century; fig. 15*C*). However, the July–September months only account for about 8 percent of the simulated recharge in a

water year (fig. 15*B*), even though almost 40 percent of water-year precipitation falls during these warm months (fig. 11*B*).

A comparison of the distribution of all median simulated groundwater infiltration results between recent historical and future periods (fig. 16) reveals projected groundwater infiltration in the upper basin to be significantly greater over the combined 2020–2099 future period than the historical period (Wilcoxon rank sum, p-value=2×10^{-6}, one tailed). In 41 of 71 (58 percent) possible future decades in this century, groundwater infiltration is expected to be greater than the 75th percentile of historical simulated groundwater infiltration. Projected groundwater infiltration in the lower Colorado River Basin across all future decades is significantly less than in the historical period (Wilcoxon rank sum, p-value=8×10^{-11}, one tailed). Of the 71 future decades in the century, projected groundwater infiltration in the lower basin is expected to be less than the 25th percentile of historical infiltration in 55 (77 percent) of the 10-year periods.

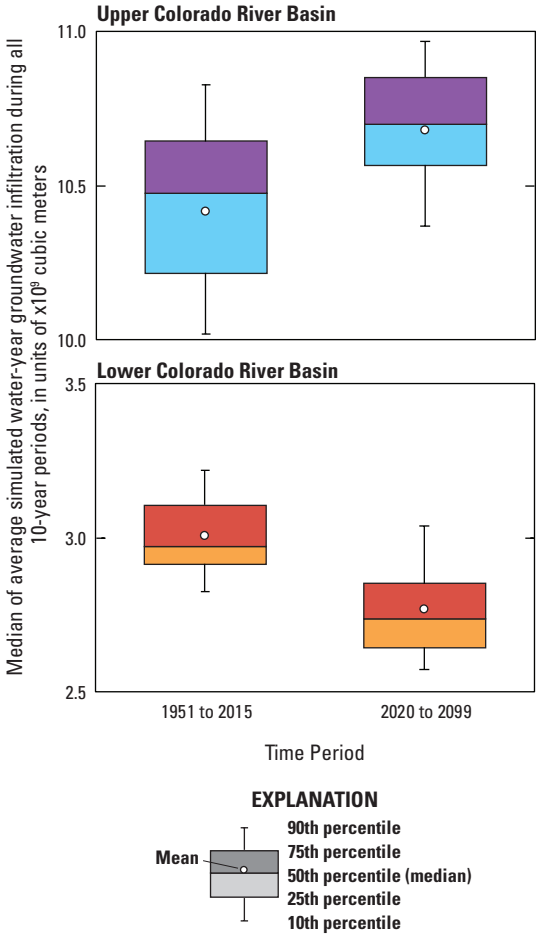

Figure 16. Boxplots comparing simulated groundwater infiltration between recent historical and future periods for the upper and lower Colorado River Basins. Upper Colorado River Basin boxplots modified from Tillman and others (2016), used with permission.

Summary and Conclusions

Groundwater discharge to streams is an important source of flow in rivers and streams in the upper Colorado River Basin. Although the importance of lower basin groundwater to flow in the Colorado River is substantially less than in the upper basin, large agricultural areas and fast-growing communities such as Phoenix and Tucson in the lower basin depend on groundwater to meet water needs. Additionally, many ecosystems in the semi-arid lower basin are sustained by groundwater discharge at spring sites. An understanding of recent trends in climate data, projected change in climate data, and projected change in groundwater infiltration in the Colorado River Basin is necessary for the sustainable management of the rivers and aquifers in the region.

Historical (1896–2019) precipitation and temperature data for the upper and lower Colorado River Basins were analyzed to better understand recent trends in climate data that may affect groundwater resources in the area. Historical data indicate multidecadal-scale cyclical patterns in precipitation in both the upper and lower basins. Although upper basin precipitation had no statistical trend over the recent historical period, the lower basin had a weak negative trend in precipitation over this period. Seasonal precipitation in the upper basin over the recent historical period was characterized by a significant increase in precipitation in the October–December months and a significant decrease in precipitation in the January–March months. Lower basin seasonal precipitation significantly decreased in the historical period in April–June and July–September months. Multidecadal-scale cyclical patterns in temperature also are observed in historical climate data in both the upper and lower basins, at least until the early 1970s. Beginning at that time, both the upper and lower basins experienced strong, monotonic positive trends in temperature. Significant positive trends in temperature are observed in the historical period (1896–2019) across all seasons for both the upper and lower basins, with greatest increases in July–September for the upper basin and in October–December for the lower basin.

Projected climate data from 97 Coupled Model Intercomparison Project phase 5 (CMIP5) climate projections across the full range of Representative Concentration Pathways (RCPs) from water years 1951 through 2099 were evaluated to understand what current global climate models are projecting about future conditions in the Colorado River Basin, and what this might mean for groundwater systems in the region. Precipitation in the upper basin is projected to increase throughout the rest of the century, rising to 6 percent above the 1951–2015 historical period by mid-21st century and to 9 percent above the historical period by the end of the century. Although not supported by recent trends in historical climate data, most of the increase in precipitation is projected to occur in January–March, during which cooler temperatures will likely provide favorable conditions for increased groundwater infiltration. Temperature in the upper basin also is projected to be above the recent historical median throughout

the rest of the century, with steady warming in decadal average temperatures expected until the last quarter of this century. Warming is projected during all seasons, a projection supported by positive temperature trends in the historical data.

In contrast to the upper basin, precipitation in the lower basin is projected to be the same as, or slightly less than, the 1951–2015 recent historical period throughout most of the rest of this century. For the seasonal periods with the greatest contribution to water-year precipitation, October–December and January–March are projected to be less than during the historical period whereas July–September precipitation is projected to be slightly greater than during the historical period. Projected increase in July–September precipitation in the lower basin is unlikely to benefit groundwater systems as higher temperatures and resulting higher PET rates during this season would likely limit additional available water for groundwater infiltration. Like projected temperature in the upper basin, temperature in the lower basin also is projected to be above the recent historical median throughout the rest of the century. Temperature (through analysis of PET) is projected to increase across all seasons in the lower basin, with the greatest increase in both the October–December and January–March months. Increases in temperature during the cooler October–December and January–March months combined with projected decreases in precipitation during these same periods would be expected to result in a decrease in the amount of available water for groundwater infiltration. Comparing median projections for all future decades with median results from all historical decades, future precipitation is expected to be greater than that of the past in the upper basin, whereas no significant difference is projected for precipitation in the lower basin. Significant increases are expected in temperature in both the upper and lower basins.

Projected precipitation and temperature results from the 97 CMIP5 climate projections were used as input in a Soil-Water Balance (SWB) groundwater infiltration model for the Colorado River Basin. SWB simulation results indicate that the upper Colorado River Basin is expected to experience mostly decades of above-historical-average groundwater infiltration through the end of the 21st century. An increase is projected in January–March groundwater infiltration and a decrease is projected in April–June infiltration, the two seasons that account for about 95 percent of water-year infiltration. For the lower Colorado River Basin, simulated groundwater infiltration is projected to be consistently less than the recent historical period for most of the remaining century. Decadal average groundwater infiltration is expected to decrease by as much as 16 percent below the recent historical period by 2059–2068. A comparison of the distribution of all median simulated groundwater infiltration results between recent historical and future periods indicates projected groundwater infiltration in the upper basin will be significantly greater over the combined 2020–2099 future period compared to the 1951–2015 recent historical period. Moreover, in 41 of 71 (58 percent) possible future decades in this century, groundwater infiltration is projected to be greater than the 75th percentile of historical simulated groundwater infiltration. Projected groundwater infiltration in the lower Colorado River Basin across all future decades is significantly less than in the historical period. Of the 71 future decades in the century, projected groundwater infiltration in the lower basin is expected to be less than the 25th percentile of historical infiltration in 55 (77 percent) of the 10-year periods.

Among the general climate model (GCM)-projected climate data, there is substantially more uncertainty (as shown by wider interquartile range of results) in projected precipitation than projected temperature. GCM projections generally agree on increasing temperatures in coming years in both the upper and lower basins. Important differences in projected precipitation between the upper basin (increasing precipitation) and lower basin (decreasing precipitation) largely drive the different responses of simulated groundwater infiltration in the upper (increasing infiltration) and lower (decreasing infiltration) basins. It may be useful to revisit projections in groundwater infiltration in the Colorado River Basin when more up-to-date projections of precipitation become available from the next CMIP exercise to see if current projections are still valid. Additionally, previous work in the upper Colorado River Basin (Tillman and others, 2017) indicates that projected climate and groundwater infiltration results summarized over a large basin might not be shared equally among subregions within the basin. Additional studies on important groundwater-dependent subregions within the lower Colorado River Basin may be useful.

References Cited

Anderson, D.L., 2004, History of the development of the Colorado River and “The law of the River” *in* Rogers, J.R., Brown, G.O., and. Garbrecht J.D., eds., Water Resources and Environmental History: Proceedings of the Water Resources and Environment History Sessions at Environmental and Water Resources Institute, p. 75–81, https://doi.org/10.1061/40738(140)11.

Apodaca, L.E. and Bails, J.B., 2000, Water quality in alluvial aquifers of the southern Rocky Mountains Physiographic Province, Upper Colorado River Basin, Colorado, 1997: U.S. Geological Survey Water-Resources Investigations Report 99–4222, 68 p., https://doi.org/10.3133/wri994222.

Bills, D.J., Flynn, M.E., and Monroe, S.S., 2007, Hydrogeology of the Coconino Plateau and adjacent areas, Coconino and Yavapai Counties, Arizona: U.S. Geological Survey Scientific Investigations Report 2005–5222, 101 p., 4 plates, https://doi.org/10.3133/sir20055222.

Bracken, C., 2016, Downscaled CMIP3 and CMIP5 climate projections—Addendum release of downscaled CMIP5 climate projections (LOCA) and comparison with preceding information: Bureau of Reclamation, 54 p., accessed August 26, 2020 at https://gdo-dcp.ucllnl.org/downscaled_cmip_projections/techmemo/Downscaled_Climate_Projections_Addendum_Sept2016.pdf.

Bureau of Reclamation, 2011, SECURE Water Act Section 9503(c)—Reclamation Climate Change and Water, Report to Congress: Bureau of Reclamation, 226 p., accessed August 26, 2020 at https://www.usbr.gov/climate/secure/docs/SECUREWaterReport.pdf.

Bureau of Reclamation, 2013a, Quality of water, Colorado River Basin, progress report no. 24: Bureau of Reclamation, 130 p., accessed August 26, 2020at https://www.usbr.gov/uc/progact/salinity/pdfs/PR24final.pdf.

Bureau of Reclamation, 2013b, Downscaled CMIP3 and CMIP5 climate projections—Release of downscaled CMIP5 climate projections, comparison with preceding information, and summary of user needs: Bureau of Reclamation, 116 p., accessed August 26, 2020 at https://gdo-dcp.ucllnl.org/downscaled_cmip_projections/techmemo/downscaled_climate.pdf.

Colorado River Basin Salinity Control Forum, 2013, Colorado River Basin salinity control program, briefing document: Colorado River Basin Salinity Control Program, 4 p., accessed August 26, 2020 at http://www.coloradoriversalinity.org/docs/CRBSCP%20Briefing%20Document%202013%20Feb%204.pdf.

Cook, B.I., Ault, T.R., and Smerdon, J.E., 2015, Unprecedented 21st century drought risk in the American Southwest and Central Plains: Science Advances, v. 1, no.1, e1400082, 8 p., https://doi.org/10.1126/sciadv.1400082.

Dettinger, M., Udall, B., and Georgakakos, A., 2015, Western water and climate change: Ecological Applications, v.25, no. 8, p. 2,069–2,093, https://doi.org/10.1890/15-0938.1.

Dripps, W.R., and Bradbury, K.R., 2009, The spatial and temporal variability of groundwater recharge in a forested basin in northern Wisconsin: Hydrological Processes, v. 24, no. 4, p. 383–392, https://doi.org/10.1002/hyp.7497.

Earman, S., Campbell, A.R., Phillips, F.M., and Newman, B.D., 2006, Isotopic exchange between snow and atmospheric water vapor—Estimation of the snowmelt component of groundwater recharge in the southwestern United States: Journal of Geophysical Research, v. 111, no. D9, D09302, https://doi.org/10.1029/2005JD006470.

Elias, E., Rango, A., Smith, R., Maxwell, C., Steele, C., and Havstad, K., 2016, Climate change, agriculture and water resources in the southwestern United States: Journal of Contemporary Water Resources & Education, v. 158, no. 1, p. 46–61, https://doi.org/10.1111/j.1936-704X.2016.03218.x.

Elias, E., Reyes, J., Steele, C., and Rango, A., 2018a, Diverse landscapes, diverse risks: synthesis of the special issue on climate change and adaptive capacity in a hotter, drier Southwestern United States: Climatic Change, v. 148, no.3, p. 339–353, https://doi.org/10.1007/s10584-018-2219-x.

Elias, E., Marklein, A., Abatzoglou, J.T., Dialesandro, J., Brown, J., Steele, C., Rango, A., and Steenwerth, K., 2018b, Vulnerability of field crops to midcentury temperature changes and yield effects in the Southwestern USA: Climatic Change, v. 148, no. 3, p. 403–417, https://doi.org/10.1007/s10584-017-2108-8.

Feinstein, D.T., Hunt, R.J., and Reeves, H.W., 2010, Regional groundwater-flow model of the Lake Michigan Basin in support of Great Lakes Basin water availability and use studies: U.S. Geological Survey Scientific Investigations Report 2010–5109, 379 p., https://doi.org/10.3133/SIR20105109.

Freethey, G.W., and Cordy, G.E., 1991, Geohydrology of Mesozoic rocks in the upper Colorado River Basin in Arizona, Colorado, New Mexico, Utah, and Wyoming, excluding the San Juan Basin: U.S. Geological Survey, Professional Paper 1411–C, 118 p., 6 plates, https://doi.org/10.3133/pp1411C.

Geldon, A.L., 2003a, Geology of Paleozoic rocks in the Upper Colorado River Basin in Arizona, Colorado, New Mexico, Utah, and Wyoming, excluding the San Juan Basin: U.S. Geological Survey, Professional Paper 1411–A, 112 p., 18 plates, https://doi.org/10.3133/pp1411A.

Geldon, A.L, 2003b, Hydrologic properties and ground-water flow systems of the Paleozoic rocks in the upper Colorado River Basin in Arizona, Colorado, New Mexico, Utah, and Wyoming, excluding the San Juan Basin: U.S. Geological Survey Professional Paper 1411–B, 153 p., 13 plates, https://doi.org/10.3133/pp1411B.

Gonzalez, P., Garfin, G.M., Breshears, D.D., Brooks, K.M., Brown, H.E., Elias, E.H., Gunasekara, A., Huntly, N., Maldonado, J.K., Mantua, N.J., Margolis, H.G., McAfee, S., Middleton, B.R., and Udall, B.H., 2018, Southwest, *in* Reidmiller, D.R., Avery, C.W., Easterling, D.R., Kunkel, K.E., Lewis, K.L.M., Maycock, T.K., and Stewart B.C. eds., Impacts, risks, and adaptation in the United States—Fourth National Climate Assessment, Volume II: U.S. Global Change Research Program, Washington, D.C., p. 1,101–1,184, https://doi.org/10.7930/NCA4.2018.CH25.

Hargreaves, G.H. and Samani, Z.A., 1985, Reference crop evapotranspiration from temperature, Applied Engineering in Agriculture, v. 1, no. 2, p. 96–99, https://doi.org/10.13031/2013.26773.

Havstad, K.M., Brown, J.R., Estell, R., Elias, E., Rango, A., and Steele, C., 2018, Vulnerabilities of Southwestern U.S. rangeland-based animal agriculture to climate change: Climatic Change, v. 148, no. 3, p. 371–386, https://doi.org/10.1007/s10584-016-1834-7.

Masterson, J.P., Pope, J.P., Monti, Jack, Jr, Nardi, M.R., Finkelstein, J.S., and McCoy, K.J., 2013, Hydrogeology and hydrologic conditions of the Northern Atlantic Coastal Plain aquifer system from Long Island, New York, to North Carolina: U.S. Geological Survey Scientific Investigations Report 2013–5133, 76 p., https://dx.doi.org/10.3133/sir20135133.

Miller, M.P., Susong, D.D., Shope, C.L., Heilweil, V.M., and Stolp, B.J., 2014, Continuous estimation of baseflow in snowmelt-dominated streams and rivers in the Upper Colorado River Basin— A chemical hydrograph separation approach: Water Resources Research, v. 50, no.8, p. 6,986–6,999, https://doi.org/10.1002/2013WR014939.

Meixner, T., Manning, A.H., Stonestrom, D.A., Allen, D.M., Ajami, H., Blasch, K.W., Brookfield, A.E., Castro, C.L., Clark, J.F., Gochis, D.J., Flint, A.L., Neff, K.L., Niraula, R., Rodell, M., Scanlon, B.R., Singha, K., and Walvoord, M.A., 2016, Implications of projected climate change for groundwater recharge in the western United States: Journal of Hydrology, v. 534, p. 124–138, https://doi.org/10.1016/j.jhydrol.2015.12.027.

Niraula, R., Meixner, T., Dominguez, F., Bhattarai, N., Rodell, M., Ajami, H., Gochis, D., and Castro, C., 2017, How might recharge change under projected climate change in the Western U.S.?: Geophysical Research Letters, v. 44, no. 20, p. 10,407–10,418, https://doi.org/10.1002/2017GL075421.

Pierce, D.W., Cayan, D.R., and Thrasher, B.L., 2014, Statistical downscaling using localized constructed analogs (LOCA): Journal of Hydrometeorology, v. 15, p. 2,558–2,585, https://doi.org/10.1175/JHM-D-14-0082.1.

Pierce, D.W., Cayan, D.R., Maurer, E.P., Abatzoglou, J.T., and Hegewisch, K.C., 2015, Improved bias correction techniques for hydrological simulations of climate change: Journal of Hydrometeorology, v. 16, p. 2,421–2,442, https://doi.org/10.1175/JHM-D-14-0236.1.

Prein, A.F., Holland, G.J., Rasmussen, R.M., Clark, M.P., and Tye, M.R., 2016, Running dry—The U.S. Southwest's drift to a drier climate state: Geophysical Research Letters, v. 43, no. 3, p. 1,272–1,279, https://doi.org/10.1002/2015GL066727.

PRISM Climate Group, 2019, Digital Climate Data: Oregon State University, accessed October 11, 2019, at http://prism.oregonstate.edu/.

R Core Team, 2019, R—A language and environment for statistical computing: R Foundation for Statistical Computing, Vienna, Austria. [Available online at https://www.R-project.org/.]

Robson, S.G. and Banta, E.R., 1995, Ground water atlas of the United States, segment 2, Arizona, Colorado, New Mexico, Utah: U.S. Geological Survey Hydrologic Investigations Atlas 730–C, 32 p., https://doi.org/10.3133/ha730C.

Schaller, N., Mahlstein, I., Cermak, J., and Knutti, R., 2011, Analyzing precipitation projections— A comparison of different approaches to climate model evaluation: Journal of Geophysical Research, v. 116, no. D10118, 14 p., https://doi.org/10.1029/2010JD014963.

Smith, E.A. and Westenbroek, S.M, 2015, Potential groundwater recharge for the State of Minnesota using the Soil-Water-Balance model, 1996–2010: U.S. Geological Survey Scientific Investigations Report 2015–5038, 85 p., https://dx.doi.org/10.3133/sir20155038.

Stanton, J.S., Qi, S.L., Ryter, D.W., Falk, S.E., Houston, N.A., Peterson, S.M., Westenbroek, S.M., and Christenson, S.C., 2011, Selected approaches to estimate water-budget components of the High Plains, 1940 through 1949 and 2000 through 2009: U.S. Geological Survey Scientific Investigations Report 2011–5183, 79 p., https://doi.org/10.3133/sir20115183.

Steele, C., Reyes, J., Elias, E., Aney, S., and Rango, A., 2018, Cascading impacts of climate change on southwestern US cropland agriculture: Climatic Change, v. 148, no. 3, p. 437–450, https://doi.org/10.1007/s10584-018-2220-4.

Thorne, J.H., Choe, H., Stine, P.A., Chambers, J.C., Holguin, A., Kerr, A.C., and Schwartz, M.W., 2018, Climate change vulnerability assessment of forests on the Southwest USA: Climatic Change, v. 148, no. 3, p. 387–402, https://doi.org/10.1007/s10584-017-2010-4.

Thornthwaite, C.W., 1948, An approach toward a rational classification of climate: Geographical Review, v. 38, no. 1, p. 55–94.

Thornthwaite, C.W. and Mather, J.R., 1957, Instructions and tables for computing potential evapotranspiration and the water balance: Centerton, N.J., Laboratory of Climatology, Publications in Climatology, v. 10, no. 3, p. 185–311.

Tillman, F.D, Gangopadhyay, S., and Pruitt, T., 2016, Changes in groundwater recharge under projected climate in the upper Colorado River Basin: Geophysical Research Letters, v. 43, p. 6,968–6,974, https://doi.org/10.1002/2016GL069714.

Tillman, F.D, 2017, Soil-water balance groundwater recharge model results for the upper Colorado River Basin: U.S. Geological Survey data release, https://doi.org/10.5066/F7ST7MX7.

Tillman, F.D, Gangopadhyay, S., and Pruitt, T., 2017, Changes in projected spatial and seasonal groundwater recharge in the upper Colorado River Basin: Groundwater, v. 55, p. 506–518, https://doi.org/10.1111/gwat.12507.

Tillman, F.D, Gangopadhyay, S., and Pruitt, T., 2019, Soil-water balance groundwater infiltration model results for the Lower Colorado River Basin: U.S. Geological Survey data release, https://doi.org/10.5066/P9VLU0O6.

U.S. Geological Survey, 2003, Principal aquifers of the 48 conterminous United States, Hawaii, Puerto Rico, and the U.S. Virgin Islands: U.S. Geological Survey Unnumbered Series, https://doi.org/10.3133/70046037.

U.S. Geological Survey, 2017, USGS Water Data for the Nation: U.S. Geological Survey National Water Information System database, accessed July 2017 at http://waterdata.usgs.gov/nwis/.

Van Vuuren, D.P., Edmonds, J., Kainuma, M. Riahi, K., Thomson, A., Hibbard, K., Hurtt, G.C., Kram, T., Krey, V., Lamarque, J.F., Masui, T., Meinshausen, M., Nakicenovic, N., Smith, S.J., and Rose, S.K., 2011, The representative concentration pathways— An overview: Climatic Change, v. 109, p. 5–31, https://doi.org/10.1007/s10584-011-0148-z.

Vose, R.S., Applequist, S., Squires, M., Durre, I., Menne, M.J., Williams, C.N., Fenimore, C., Gleason, K., and Arndt, D., 2014a, Gridded 5km GHCN-Daily Temperature and Precipitation Dataset (nCLIMGRID): NOAA National Centers for Environmental Information, https://doi.org/10.7289/V5SX6B56.

Vose, R.S., Applequist, S., Squires, M., Durre, I., Menne, M.J., Williams, C.N., Fenimore, C., Gleason, K., and Arndt, D., 2014b, Improved historical temperature and precipitation time series for U.S. climate divisions: Journal of Applied Meteorology and Climatology, v. 53, p. 1,232–1,251, https://doi.org/10.1175/JAMC-D-13-0248.1.

Westenbroek, S.M., Engott, J.A., Kelson, V.A., and Hunt, R.J., 2018, SWB Version 2.0—A soil-water-balance code for estimating net infiltration and other water-budget components: U.S. Geological Survey Techniques and Methods, book 6, chap. A59, 118 p., https://doi.org/10.3133/tm6A59.

Whitehead, R.L., 1996, Ground water atlas of the United States, segment 8, Montana, North Dakota, South Dakota, Wyoming: U.S. Geological Survey Hydrologic Investigations Atlas 730–I, 24 p., http://pubs.usgs.gov/ha/ha730/gwa.html.

Wood, A. W., Maurer, E. P., Kumar, A., and Lettenmaier, D. P., 2002, Long-range experimental hydrologic forecasting for the Eastern United States: Journal of Geophysical Research, v. 107, no.D20, p. ACL6-1–ACL6-15, https://doi.org/10.1029/2001JD000659.

Wood, A. W., Leung, L. R., Sridhar, V., and Lettenmaier, D. P., 2004, Hydrologic implications of dynamical and statistical approaches to downscaling climate model outputs: Climatic Change, v. 62, p.189–216, https://doi.org/10.1023/B:CLIM.0000013685.99609.9e.

Appendix 1. Computational Details and Limitations of the Soil-Water Balance Groundwater Infiltration Model

The Soil-Water-Balance (SWB) groundwater infiltration model (Westenbroek and others, 2018) estimates spatial and temporal variations in groundwater infiltration by calculating water balance components at daily time steps. SWB follows a modified Thornthwaite-Mather soil-water-balance accounting approach (Thornthwaite, 1948; Thornthwaite and Mather, 1957). Sources and sinks of water within each grid cell in the model domain are estimated based on climate data and landscape characteristics, and groundwater infiltration is then estimated as the difference between the change in soil moisture and these sources and sinks (equation 1 in the main text).

SWB infiltration simulations require spatially gridded datasets for land cover, hydrologic soil group, available soil-water capacity, overland flow direction, daily maximum temperature, daily minimum temperature, and daily precipitation. SWB simulations also require tabular information including runoff curve numbers, interception values, vegetation rooting depths, and maximum daily recharge values for each combination of hydrologic soil group and land-cover type. In SWB simulations, inflow to a model cell is surface flow from adjacent cells, which is calculated using the National Resources Conservation Service (NRCS) curve number rainfall-runoff relation. Runoff flow direction is determined using a flow-direction grid derived from a digital elevation model. Interception is a user-specified amount of precipitation that is trapped and used by vegetation and outflow from a cell is calculated in the same manner as inflow. Several methods are available for estimating potential evapotranspiration (PET) in the SWB model, from which actual evapotranspiration (AET) is calculated. For Colorado River Basin simulations, the Hargreaves-Samani (Hargreaves and Samani, 1985) method is used as it produces spatially variable estimates of PET from spatially varying minimum and maximum air temperature data for each daily time step:

$$\mathrm{PET}=0.0135\times RS\times(T+17.8) \text{ with } RS=KRS\times RA\times TD^{0.5}$$

where

PET is potential evapotranspiration, in units of equivalent water evaporation;

RS is incoming solar radiation, in units of equivalent water evaporation;

T is mean air temperature, in degrees Celsius;

K_{RS} is a calibration coefficient;

RA is extraterrestrial radiation, in units of equivalent water evaporation; and

TD is the measured air temperature range, in degrees Celsius (Hargreaves and Samani, 1985).

Extraterrestrial radiation is estimated as a function of latitude and the day of year (Allen and others, 1998). Computation of soil moisture in equation 1 requires several intermediary values. First, PET is subtracted from precipitation (P) for all grid cells. If P<PET, then there is a potential deficiency of water and accumulated potential water loss (APWL) is computed as the running sum of daily P–PET values during times when P<PET. Soil moisture is estimated using current AWPL in the Thornthwaite-Mather relation that describes the nonlinear relation between soil moisture and APWL. AET is then equal to only the amount of water that can be extracted from the soil. If P > PET, then a potential surplus of water exists and AET is equal to PET. Soil moisture is then calculated by adding P–PET directly to the previous day's soil-moisture value. If the new soil moisture value is less than the maximum water-holding capacity of the soil, which is estimated as the product of the root-zone depth and available soil water capacity, then the Thornthwaite-Mather relation is used to back-calculate a reduced APWL. If the new soil moisture value is greater than the maximum water-holding capacity of the soil, then excess soil-moisture becomes recharge, soil moisture is set to the maximum water-holding capacity, and AWPL is set to zero.

For Colorado River Basin SWB recharge simulations, all spatially gridded input datasets were resampled to the same cell size and geographic coordinate system as the 1/8° × 1/8° (latitude × longitude) climate data. Detailed descriptions of the sources, manipulation, and resampling of SWB model inputs for upper Colorado River Basin infiltration simulations are provided in Tillman (2015).

Climate change is expressed in SWB infiltration simulations (equation 1) through the computation of AET (mean temperature) and through precipitation input. The Colorado River Basin SWB model does not include changes in land use that may take place in the future or simulate changes in stomatal conductance or leaf area in a carbon dioxide enriched atmosphere (Eckhardt and Ulbrich, 2003; Holman and others, 2012). Only direct effects of climate change are evaluated in the Colorado River Basin SWB infiltration results.

Although the SWB infiltration model has been shown to provide reasonable basin-scale estimates of groundwater infiltration, SWB assumptions and limitations should be considered when evaluating simulation results (Westenbroek and others, 2018). The daily time step of the SWB model allows short-term surpluses of water to become groundwater infiltration, but also necessitates that overland-flow routing of runoff either infiltrate in cells downslope or be routed out

of the model domain on the same day in which it originated. In addition, depth to the top of the aquifer surface is not considered in SWB simulations, and there may be substantial time of travel through the unsaturated zone. Use of the NRCS curve number method to estimate runoff in SWB simulations introduces limitations, including that the method was developed to evaluate floods and was not designed to simulate daily flows of ordinary magnitude. Studies show that the curve number is not constant but may vary from event to event (Westenbroek and others, 2010). Finally, there are numerous methods for estimating evapotranspiration, each with its own benefits, limitations, uncertainties, and data requirements. This study uses the Hargreaves-Samani (Hargreaves and Samani, 1985) method for PET, in which climate changes are reflected only in the daily air temperature range. More complex evapotranspiration relations require additional data that may include relative humidity, wind speed, and percentage of actual to possible daily sunshine hours, among others (Westenbroek and others, 2010).

References Cited

Allen, R.G., Pereira, L.S., Raes, D., and M. Smith, 1998 (with errata 2006), Crop evapotranspiration—Guidelines for computing crop water requirements: FAO Irrigation and Drainage Paper 56, Food and Agricultural Organization of the United Nations, Rome, Italy, 333 p., accessed February 8, 2017, at http://www.fao.org/docrep/x0490e/x0490e00.htm#Contents.

Eckhardt, K. and Ulbrich, U., 2003, Potential impacts of climate change on groundwater recharge and streamflow in a central European low mountain range: Journal of Hydrology, v. 284, p. 244–252, https://doi.org/10.1016/j.jhydrol.2003.08.005.

Hargreaves, G.H. and Samani, Z.A., 1985, Reference crop evapotranspiration from temperature: Applied Engineering in Agriculture, v. 1, no. 2. p. 96–99, https://doi.org/10.13031/2013.26773.

Holman, I.P., Allen, D.M., Cuthbert, M.O., and Goderniaux, P., 2012, Towards best practice for assessing the impacts of climate change on groundwater: Hydrogeology Journal, v. 20, p. 1–4, https://doi.org/10.1007/s10040-011-0805-3.

Thornthwaite, C.W., 1948, An approach toward a rational classification of climate: Geographical Review 38, no. 1, p. 55–94, https://doi.org/10.2307/210739.

Thornthwaite, C.W. and Mather, J.R., 1957, Instructions and tables for computing potential evapotranspiration and the water balance: Publications in Climatology, v. 10, no. 3, p. 185–311.

Tillman, F.D., 2015, Documentation of input datasets for the soil-water balance groundwater recharge model for the Upper Colorado River Basin: U.S. Geological Survey Open-File Report 2015–1160, 17 p., https://doi.org/10.3133/ofr20151160.

Westenbroek, S.M., Kelson, V.A., Hunt, R.J., and Bradbury, K.R., 2010, SWB—A modified Thornthwaite-Mather soil-water balance code for estimating groundwater recharge: U.S. Geological Survey Techniques and Methods 6–A31, 60 p., https://doi.org/10.3133/tm6A31.

Westenbroek, S.M., Engott, J.A., Kelson, V.A., and Hunt, R.J., 2018, SWB Version 2.0—A soil-water-balance code for estimating net infiltration and other water-budget components: U.S. Geological Survey Techniques and Methods, book 6, chap. A59, 118 p., https://doi.org/10.3133/tm6A59.

Moffett Publishing Service Center, California
Manuscript approved for publication September 16, 2020
Edited by John Mark Brigham
Layout and design by Kimber Petersen
Illustration support by JoJo Mangano

ISSN 2328-0328 (online)
https://doi.org/10.3133/sir20205107